

NUREG/CR-3776

SAND83-1960

AN

Printed July 1984

Testing of Safety-Related Nuclear Power Plant Equipment at the Central Receiver Test Facility

Vincent J. Dandini, John J. Aragon

Prepared by
Sandia National Laboratories
Albuquerque, New Mexico 87185 and Livermore, California 94550
for the United States Department of Energy
under Contract DE-AC04-76DP00785



8409110074 840731
PDR NUREG
CR-3776 R PDR

Prepared for
U. S. NUCLEAR REGULATORY COMMISSION

NOTICE

This report was prepared as an account of work sponsored by an agency of the United States Government. Neither the United States Government nor any agency thereof, or any of their employees, makes any warranty, expressed or implied, or assumes any legal liability or responsibility for any third party's use, or the results of such use, of any information, apparatus product or process disclosed in this report, or represents that its use by such third party would not infringe privately owned rights.

Available from
GPO Sales Program
Division of Technical Information and Document Control
U.S. Nuclear Regulatory Commission
Washington, D.C. 20555

and

National Technical Information Service
Springfield, Virginia 22161

NUREG/CR-3776
SAND83-1960
AN

TESTING OF SAFETY-RELATED NUCLEAR POWER
PLANT EQUIPMENT AT THE CENTRAL RECEIVER
TEST FACILITY

Vincent J. Dandini
John J. Aragon

July 1984

Sandia National Laboratories
Albuquerque, NM 87185
Operated by
Sandia Corporation
for the
U. S. Department of Energy

Prepared for
Containment Systems Research Branch
Division of Accident Evaluation
Office of Nuclear Regulatory Research
and
Chemical Engineering Branch
Division of Engineering
Office of Nuclear Reactor Regulation
Washington, D. C. 20555
Under Memorandum of Understanding DOE 40-550-75
NRC Fin Nos. A-1270 and A-1306

ABSTRACT

The use of a solar energy facility for simulating the thermal environment (heat flux) produced as a result of hydrogen burns in a full-scale reactor containment building is described. Using a heat flux profile developed from calculations performed by the HECTR computer code, the Central Receiver Test Facility simulated the multiple burn thermal environment which HECTR predicted would result from the deliberate ignition of hydrogen generated by an S₂D accident. Functioning specimens of reactor monitoring and safety system equipment were exposed to this environment. Results of the equipment performance and temperature response are presented.

CONTENTS

	<u>Page</u>
Executive Summary	1
1.0 INTRODUCTION	4
2.0 THE HYDROGEN BURN THERMAL ENVIRONMENT	5
3.0 THE TEST FACILITY	7
4.0 THE CRIF FLUX PROFILE	12
5.0 PROFILE AND FACILITY TESTING	19
6.0 TEST SPECIMENS, INSTRUMENTATION AND TEST CONFIGURATION	23
6.1 NEMA Box	23
6.2 Cable and Terminal Blocks	23
6.3 Hydrogen Ignitor	24
6.4 Solenoid Valves	26
6.5 Differential Pressure Transmitter	29
6.6 Pressure Transmitter	32
7.0 TEST PROCEDURE	34
8.0 RESULTS	36
8.1 NEMA Box	36
8.2 Terminal Blocks and Cable	36
8.3 Hydrogen Ignitor	38
8.4 Solenoid Valves	40
8.5 Foxboro Differential Pressure Transmitter	44
8.6 Barton Pressure Transmitter	58
9.0 CONCLUSIONS	68
References	73

LIST OF FIGURES

<u>Figure</u>	<u>Page</u>
2-1 Effect of Volume on Heat Pulse Duration	6
3-1 The Central Receiver Test Facility (CRTF).	8
3-2 The CRTF Shutter	9
3-3 A Typical CRTF Heliostat	10
4-1 HECTR-Calculated Heat Flux	13
4-2 Calculated-CRTF Pulse Comparison	17
5-1 CRTF Multiple Burn Simulation	21
5-2 Comparison of HECTR-Calculated and CRTF-Produced Temperature Rises for a Multiple Burn	22
6-1 Hydrogen Ignitor Assembly	25
6-2 New ASCO Solenoid Valve	27
6-3 Solenoid Valve Function Test Set-Up	28
6-4 Foxboro Differential Pressure Transmitter	30
6-5 Transmitter Test Set-Up	31
6-6 Barton Pressure Transmitter	33
8-1 NEMA Box Temperatures	37
8-2 Hydrogen Ignitor Temperatures	39
8-3 Solenoid Valve Operation Signal	41
8-4 New Solenoid Valve Temperatures	42
8-5 Final New Valve Temperatures	43
8-6 FITS Valve Solenoid Housing Temperature Response	45
8-7 Foxboro Transmitter Temperature Responses (Non-Electronic Components)	46

LIST OF FIGURES (Cont.)

<u>Figure</u>	<u>Page</u>
8-8 Foxboro Transistor Temperature Responses . . .	47
8-9 Foxboro Transmitter Performance	49
8-10 Foxboro Pretest Signal Output	51
8-11 Foxboro Posttest Signal Output at Elevated Temperature	53
8-12 Foxboro Posttest Signal Output at Ambient Temperature	54
8-13 Foxboro Pre and Posttest Signal Comparison	55
8-14 Effect of Temperature on Foxboro Signal Voltage at Test Pressure (7 psi)	57
8-15 Pretest Barton Transmitter Calibrations . . .	59
8-16 Barton Transmitter Voltages	60
8-17 Barton Transmitter Casing Temperatures . . .	62
8-18 Barton Electronic Component Temperatures . .	63
8-19 Posttest Barton Calibration at Elevated Temperature	64
8-20 Posttest Barton Calibration at Ambient Temperature	65
8-21 Barton Transmitter Calibration Comparison . .	67

LIST OF TABLES

<u>Table</u>		<u>Page</u>
5-1	Comparison of HECTR-Calculated and CRTF-Produced Temperature Rises	20
8-1	NEMA Box Temperature Rises	36
8-2	New Solenoid Valve Temperature Responses . .	40
8-3	Foxboro Transmitter Temperature Rises	48
8-4	Foxboro Transmitter Calibration Equations . .	52
8-5	Foxboro Signal Comparison at 48.3 kPa (7 psi) Differential Pressure	56
8-6	Barton Transmitter Temperature Rises	61
8-7	Barton Transmitter Calibration Equations . .	66
9-1	Generalized Results of CRTF Hydrogen Burn Simulation	70

ACKNOWLEDGMENTS

The HBS program incorporates the efforts of many individuals at Sandia. The authors wish to acknowledge the contributions of the following Sandia personnel to the CRTF testing: Ben Bader and Lou Cropp, supervisors of Sandia Division 6445; Bill McCulloch, HBS project manager; and Dave Furgal for his advice in instrumenting the test specimens; Beth Richards for her counsel on the capabilities of the CRTF; Allen Camp and Susan Dingman who helped develop HECTR and generated the heat flux profiles; and Bob Edgar, Debbie Risvold and Arlene Vance of the CRTF for their assistance in conducting the tests.

EXECUTIVE SUMMARY

The hydrogen burn which occurred during the Three Mile Island accident has raised concern that a similar event in other containment buildings could compromise the ability of that structure to prevent the release of fission products to the environment. One method suggested for preventing such an occurrence is the deliberate ignition of the hydrogen at concentrations low enough to preclude potentially damaging overpressures. This method results in the combustion of hydrogen at lower concentrations (resulting in lower environmental temperatures) than might occur without deliberate ignition. Deliberate ignition, however, may expose safety-related equipment to high temperature gases and the effect of this environment must be assessed.

The primary objective of the Hydrogen Burn Survival (HBS) program at Sandia National Laboratories is to develop a basis for determining the overall response of safety-related equipment to the hydrogen burn environment. Based on this determination, the need to include the hydrogen burn environment in equipment qualification requirements can be assessed. Pursuant to this objective two of the goals of the HBS program are to:

1. Develop a method to simulate the thermal environment (heat flux) inside a reactor containment building resulting from the deliberate ignition of hydrogen and
2. Evaluate how actual pieces of safety related equipment are affected when exposed to this simulated environment.

The characteristics of hydrogen combustion in closed volumes are such that the severity of the resulting environment is dependent on the volume in which the burn occurs. Burns in full-sized containment volumes result in heat flux pulses which remain at high levels for much longer periods of time than would similar burns in vessels of the relatively small size currently being used in most hydrogen combustion studies. Lacking a containment-sized experimental vessel, a technique was developed employing the Central Receiver Test Facility to simulate the hydrogen burn thermal environment.

The thermal environment in the lower compartment of an ice condenser containment building resulting from a series of deliberate hydrogen burns precipitated by an S₂D accident was characterized by the HECTR computer code. Ignition was taken to occur at 8 volume-percent hydrogen concentration. Using specimen absorptance values for solar and infrared radiation, a solar heat flux profile corresponding

to the HECTR calculated flux profile was determined. Due to differences in specimen solar and IR absorptivities and the simulation of convective heat flux using solar radiation, the solar flux profile differs somewhat from the total flux profile (convection plus radiation) predicted by HECTR. However, the heat input to the test specimens was the same. Exposure of an experimental specimen to the solar flux profile produced a temperature rise which agreed very closely with that calculated by HECTR for the same specimen. For the accident scenario considered (S₂D), HECTR predicted seven similar burns. This multiple burn profile was simulated by repetition of the same pulse seven times in the simulation tests.

The equipment tested was:

1. A large NEMA-4 electrical enclosure,
2. Four samples of electrical cable, three of which were qualified for nuclear application,
3. Two nuclear-qualified terminal blocks, a General Electric EB25A0636 and a Westinghouse S-542247,
4. A hydrogen ignitor assembly,
5. Two nuclear-qualified ASCO solenoid valves. One was in new condition and the other had been subjected to several hydrogen burn tests in Sandia's FITS facility,
6. A nuclear qualified Barton model 763 pressure transmitter and,
7. A nuclear qualified Foxboro model N-E13DM differential pressure transmitter.

All specimens were in operation during the tests. The electrical cables had an applied potential of 8 volts and each was connected in series with a 500 ohm resistor. They were mounted in the test facility using the terminal blocks. The hydrogen ignitor was activated. Both solenoid valves were attached to a pressure system and cycled every four seconds while valve operation was monitored with a pressure switch. The Barton transmitter was pressurized to 15.5 MPa (2250 psi) and the instrument pressure signal monitored throughout testing. The Foxboro transmitter was pressurized to a differential pressure of 48.3 kPa (7 psi) and its pressure signal monitored. Temperatures of important specimen components and selected voltages were also monitored throughout testing.

All specimens performed normally throughout the tests. A small blister formed on the unqualified cable but no electrical failure occurred in the cable or terminal block samples. The highest temperatures observed were on the large NEMA enclosure and the similar small box housing the hydrogen ignitor transformer and glow plug. Temperature measurements of the air and the components inside these enclosures indicate that components contained inside them would not be harmed. Both solenoid valves cycled continuously with no sticking. The Barton transmitter gave a steady signal corresponding to its pre-test calibration throughout testing and posttest checks at several different pressures, which indicated that it remained in calibration over its operating range.

The only adverse effect noted was a change in calibration of the Foxboro transmitter. During testing the signal was steady and differed from the pretest calibration value for the test pressure by slightly less than 3 percent. A calibration check conducted shortly after test completion, while the instrument was still at elevated temperature, showed significant differences at the lower end of the pressure span (approximately 20 percent at 3 psi). Several days later, after the transmitter had cooled back to ambient temperature, the calibration had returned nearer to, but not coinciding with, the pretest calibration.

The conclusions of this report are:

1. The Central Receiver Test facility is a valid simulator of HECTR-calculated heat fluxes of the hydrogen burn thermal environment.
2. The Foxboro N-E13DM differential pressure transmitter is subject to calibration changes at elevated temperatures. These changes occur at temperatures that are within the manufacturer's stated bounds of operation.
3. Except for the Foxboro calibration changes noted above, the thermal environment (as defined by HECTR) in the lower compartment of an ice condenser containment building resulting from a series of deliberate hydrogen burns precipitated by an S₂D accident does not, by itself, appear to threaten safety-related equipment having thermal characteristics similar to the specimens considered in this series of tests.

1.0 INTRODUCTION

Among the many events that took place during the accident at Three Mile Island in March of 1979 was a single hydrogen burn which caused pressure in the unit 2 containment building to rise rapidly to a peak of 193 kPa (28 psi).¹ The strength of the TMI structure was such that its integrity was not threatened. This pressure spike has, however, raised concerns that a similar event in a reactor building of different design, such as an ice condenser containment, could jeopardize the ability of that structure to prevent the release of fission products to the environment.

One method proposed to prevent such an occurrence is the deliberate ignition of the hydrogen before it accumulates to concentrations which, if burned, might threaten containment integrity. In this way, large pressure pulses caused by the combustion of high concentrations of hydrogen can be avoided. However, the thermal environment resulting from this deliberate ignition may have the undesirable side effect of degrading equipment necessary to maintain the reactor in a safe shutdown condition and monitor plant conditions.

The primary objective of the Hydrogen Burn Survival (HBS) program at Sandia National Laboratories is to develop a basis for determining the overall response of safety-related equipment to the hydrogen burn environment. Based on this determination, the need to include the hydrogen burn environment in equipment qualification requirements can be assessed.

Among the subsidiary goals of the program are the establishment of the capability to simulate the thermal environment resulting from the deliberate ignition of hydrogen inside a containment building, and to examine the thermal and operational responses of selected items of safety equipment during and after exposure to the simulated environment.

The present report addresses these goals as they relate to nuclear power plants with ice condenser containment buildings.

2.0 THE HYDROGEN BURN THERMAL ENVIRONMENT

Experiment and analysis have shown that the thermal environment resulting from the rapid combustion of hydrogen in closed volumes takes the form of a pulse of heat energy.² A short time prior to the initiation of hydrogen release, gas temperatures (and thus heat fluxes) to which safety-related equipment is exposed are elevated due to conditions resulting from the loss of coolant accident (LOCA) which precedes hydrogen generation. As hydrogen is first released the fluxes remain at this elevated, but relatively low, level until hydrogen has accumulated to a sufficiently high concentration to be ignited by an ignition source. At ignition, the gas temperatures and heat fluxes, both convective and radiant, rise rapidly to some peak value and then as gas temperatures decline, the fluxes slowly decay to preignition levels. During this decay, hydrogen continues to be generated and when an ignitable concentration has again been achieved another burn occurs. This succession of burns continues until the supply of combustible hydrogen or oxygen has been exhausted. Alternatively, if the hydrogen release rate is sufficiently high, the hydrogen can ignite at or near its release point and burn continuously in a standing flame. This scenario is not considered in this report.

Analysis and experiment have also shown that the duration of the heat flux pulse is dependent upon the volume of the vessel in which the burn occurs.² Gas temperatures, and thus flux levels, remain elevated for significantly longer times in containment-sized volumes (34,000 to 76,000 m³), than in volumes characteristic of experimental facilities currently employed in hydrogen burn studies (less than 5 m³ to 2,100 m³). Figure 2-1 compares measured gas temperatures in the Variable Geometry Experimental System (VGES) at SNL and the analytically determined gas temperatures in the upper compartment of an ice condenser containment building with sprays inoperative.²

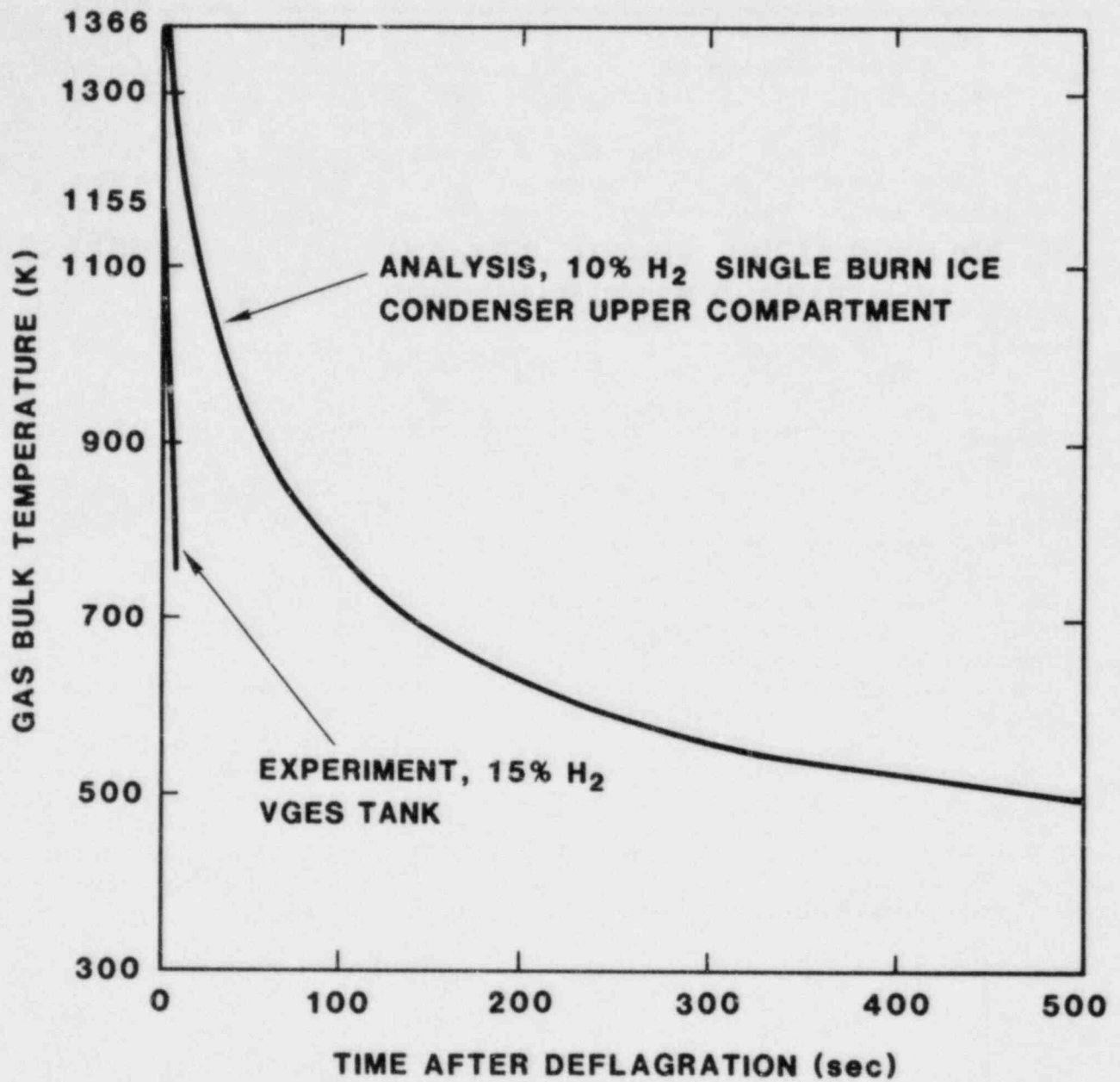


Figure 2-1 Effect of Volume on Heat Pulse Duration

3.0 THE TEST FACILITY

Lacking a containment-sized vessel in which to conduct actual hydrogen burns, it was necessary to identify a facility which could simulate, as closely as possible, the predicted heat flux profiles resulting from the thermal environment produced by the deliberate ignition of hydrogen in a reactor containment building. Two appropriate facilities exist at Sandia. One, the Radiant Heat Facility (RHF), uses electric quartz lamps to produce the thermal flux. The other, the Central Receiver Test Facility (CRTF), uses focused mirror arrays (heliostats) to concentrate sunlight on a test specimen mounted in a tower. The CRTF was chosen for its heat flux pulse and multiple burn simulation capability. Additional attractive features include rapid turn-around between tests, its large test area (1 m^2) which permits the testing of large specimens or several smaller ones, good data acquisition, initial facility availability, and cost effectiveness.

The CRTF is shown in Figure 3-1. It consists of four basic components:³ the tower, the heliostat field, a shutter, and the control room.

The tower is a large concrete structure 61 m (200 ft) high housing several test bays and the remote portion of the data acquisition system which links the experiment instrumentation to the data acquisition computers in the control room. The HBS experiments were conducted at the 43 m (140 ft) level in a test bay equipped with a shutter.

The heliostat field consists of 222 separate heliostats (one of which is shown in Figure 3-3) having individual flux-on-target capabilities ranging from 5 kW/m^2 to 13 kW/m^2 depending on its location within the field. The total thermal power of the heliostat array is slightly over 5 MW spread over a spot 2 m in diameter. The HBS testing used seven heliostats focused on the closed shutter to achieve the required peak flux levels.

The shutter, shown in Figure 3-2 is a water cooled device which, when opened, simulates the rapid rise in heat flux which is characteristic of the early stages of the pulse immediately after hydrogen ignition occurs. It is pneumatically driven and actuated simultaneously with the data acquisition computer program at the start of a test. At the end of a pulse the same program automatically closes the shutter to allow repositioning of the heliostats for the next pulse.

The control room is located in a separate building behind the heliostat field. It houses five computers, collectively known as the Master Control System (MCS), which control heliostat motion and other facility hardware;

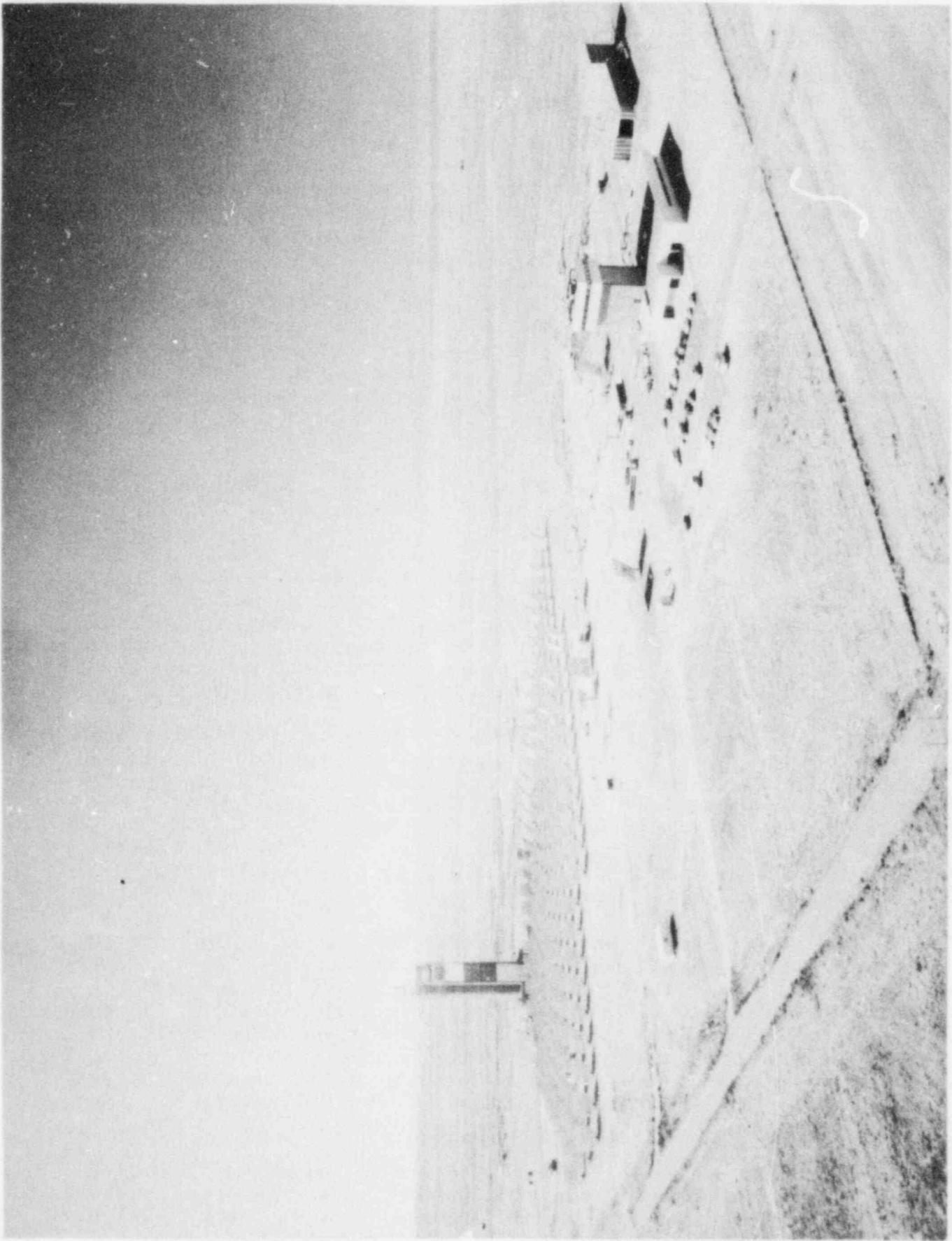


Figure 3-1 The Central Receiver Test Facility (CRTF)

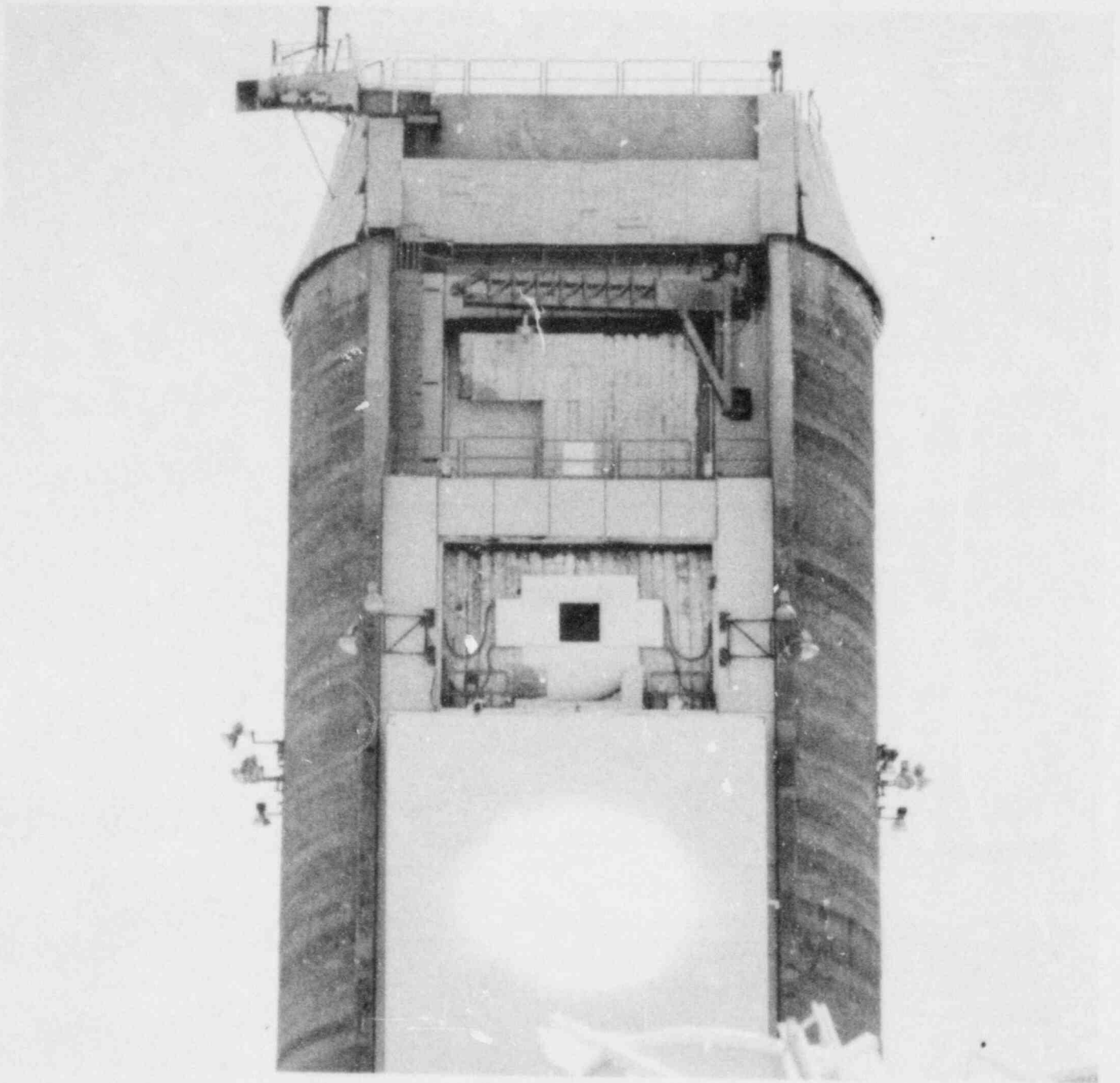


Figure 3-2 The CRTF Shutter

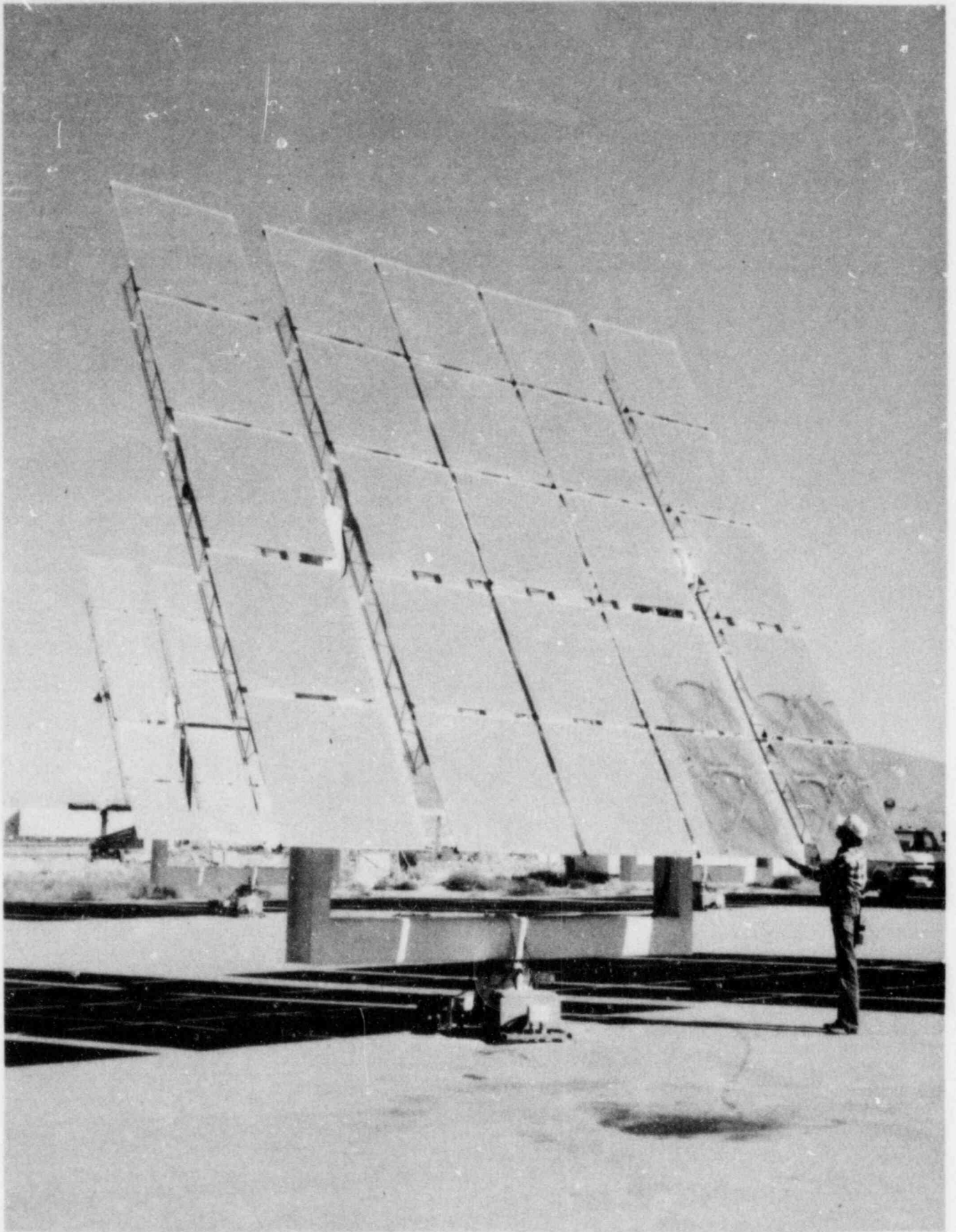


Figure 3-3 A Typical CRTF Heliostat

acquire, process, store and display data; and monitor CRTF performance. The control room also houses a special closed circuit television system which allows observation of test specimens during testing. The brilliance of concentrated sunlight prohibits direct visual observation.

A more complete description of the CRTF and its components is given in Reference 3.

4.0 THE CRTF FLUX PROFILE

Since empirical data which describes the heat flux vs. time profiles resulting from hydrogen burns in full sized containments does not exist, the profiles simulated in these experiments were calculated using the HECTR code.⁴ This code was developed at Sandia for analysis of the pressure and temperature environment inside containment volumes before, during, and after hydrogen deflagrations.

The accident scenario chosen was the S₂D event, a small break (less than 5 cm or 2 inches in diameter) LOCA with failure of the Emergency Core Cooling System (ECCS). This event was chosen for its similarity to the TMI-2 accident, relatively high probability of occurrence as determined by probabilistic risk assessments (PRA's),⁵ and because it is used throughout industry when considering hydrogen producing events. The ignition criterion, i.e., the hydrogen concentration at which combustion is assumed to have initiated, was 8 volume-percent hydrogen. Combustion was taken to be 100 percent complete. Fans and sprays were taken to be operational. The location considered was the lower compartment of the Sequoyah containment building, an ice condenser containment. This compartment was chosen because the environment there is a conservative representation of the conditions in both the lower compartment and dead-ended regions, which, taken together, house large amounts of safety-related equipment. The heat flux vs. time profile calculated by HECTR for this set of conditions is shown in Figure 4-1.

Two factors required consideration when establishing the CRTF flux profile from that calculated by HECTR. First, the CRTF does not have a convective component of heat input. For hydrogen burns in reactor containments, convection is significant. HECTR calculates that during the high flux portions of the pulse it constitutes nearly one-third of the total incident flux and during the tail portion it is the dominant heat transfer mechanism. Second, the differences in the incident radiant heat flux spectra must be considered. The CRTF employs the solar spectrum. The radiant heat environment inside a containment building is due to hot gases, primarily water vapor, resulting from the combustion of hydrogen. These hot gases radiate in the near-infrared and infrared spectrum. Both differences were addressed by considering the values for the specimen absorptivity in the solar and IR regions of the spectrum.

The requirement for accident simulation is to have the specimen absorb the same amount of heat at the CRTF as it would when subjected to the hydrogen burn environment and to do so in a transient fashion similar to that predicted by HECTR. Stated in terms of heat flux, this requirement is:

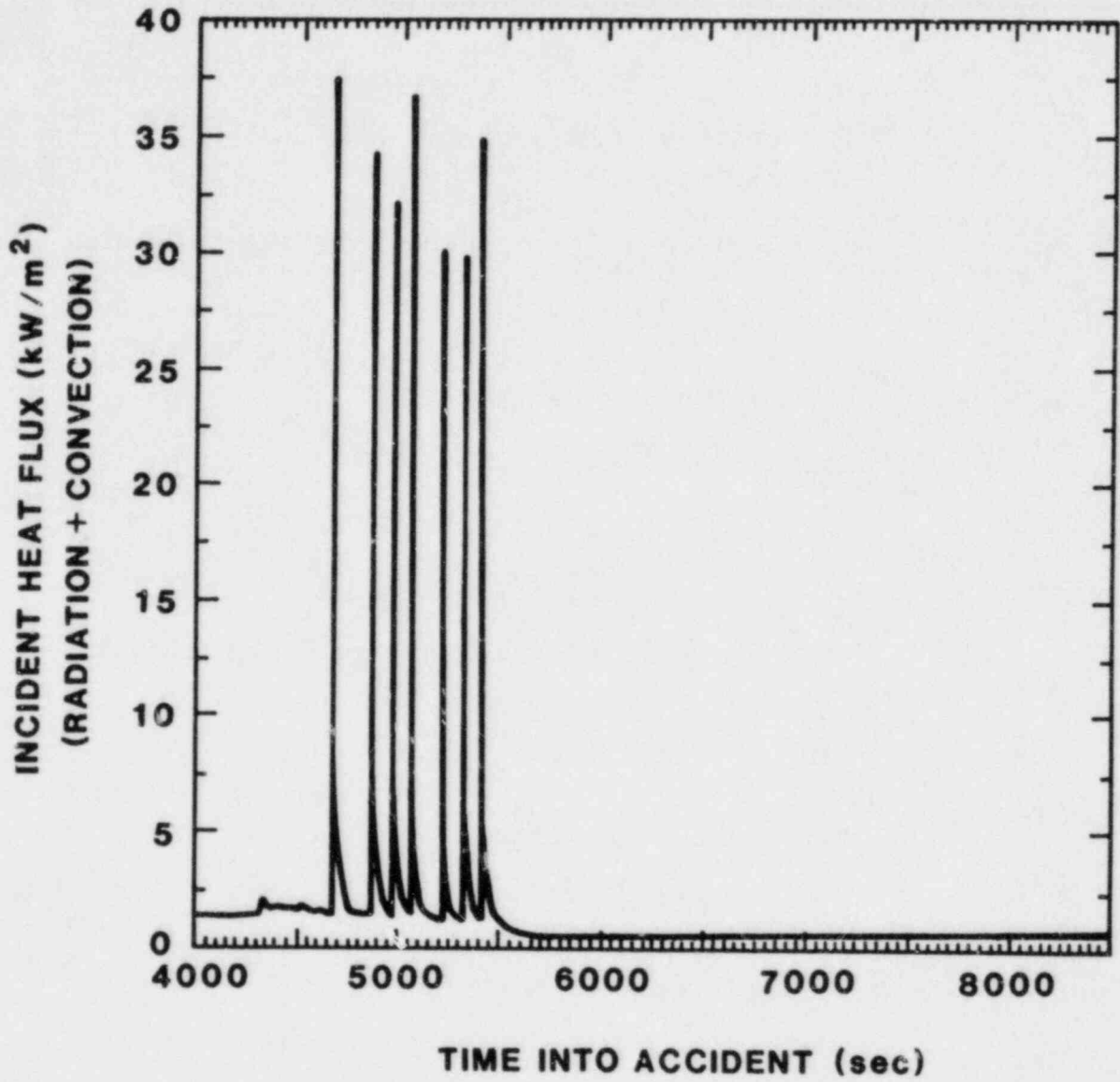


Figure 4-1 HECTR-Calculated Heat Flux

$$q''_{abs} = q''_c + \alpha_a q''_r \quad (4-1)$$

where q''_{abs} = absorbed flux

q''_c = convective flux

q''_r = radiant flux

α_a = absorptivity for the incident radiant flux spectrum due to the accident

The requirement was that a solar flux vs. time profile be established which would accomplish this.

The convective heat flux is given by:

$$q''_c = h(T_g - T_c) \quad (4-2)$$

h = convective heat transfer coefficient

T_g = temperature of the hot gas

T_c = component surface temperature

The convective flux is totally absorbed in the component. This being so, the convective flux calculated by HECTR can be simulated by solar radiation if:

$$q''_{cs} = \frac{q''_{cH}}{\alpha_s} \quad (4-3)$$

where q''_{cs} = solar simulated convective flux

q''_{cH} = HECTR-calculated convective flux

α_s = average solar absorptivity of the component

The convection correlations used to determine q_{CH}'' are standard empirically determined relationships. They^{CH} were established using geometries dissimilar to that of the interior of a reactor containment building. Thus, there is some, as yet undetermined, uncertainty in the HECTR-calculated convective flux.

The radiant component must be determined such that

$$\alpha_s q_{rs}'' = \alpha_a q_{rH}'' \quad (4-4)$$

or

$$q_{rs}'' = \left(\frac{\alpha_a}{\alpha_s} \right) q_{rH}'' \quad (4-5)$$

where q_{rs}'' = solar simulated radiant flux

q_{rH}'' = HECTR-calculated radiant flux

The sum of the solar simulated convective and radiant fluxes defines the total incident solar flux which will simulate the HECTR-calculated flux. That is,

$$q_{is}'' = q_{cs}'' + q_{rs}'' \quad (4-6)$$

where q_{is}'' = incident solar flux.

Substituting Equations (4-3) and (4-5) into (4-6), we get.

$$q_{is}'' = \left(\frac{q_{cH}''}{\alpha_s} \right) + \left(\frac{\alpha_a}{\alpha_s} \right) q_{rH}'' \quad (4-7)$$

The absorbed solar flux is given by

$$q''_{abs} = \alpha_s q''_{is} \quad (4-8)$$

As a check on requirements, we substitute Equation (4-7) into Equation (4-8):

$$q''_{abs} = \alpha_s \left(\frac{q''_{cH}}{\alpha_s} \right) + \alpha_s \left(\frac{\alpha_a}{\alpha_s} \right) q''_{rH} \quad (4-9)$$

which yields Equation (4-1) with the convective and radiant fluxes defined by HECTR. Thus, Equation (4-7) defines the incident solar flux necessary to simulate the sum of the convective and radiant terms as defined by HECTR. In the event that the absorptances are nearly equal, that is, if the absorptance is not a strong function of wavelength,

$$\alpha_a \approx \alpha_s \quad (4-10)$$

then we can let

$$q''_{rs} = q''_{rH} \quad (4-11)$$

and little or no change need be made to the HECTR-calculated radiant flux. Values for q''_{cH} and q''_{rH} were obtained from HECTR. Values of α_a and α_s were determined for the test specimens by the Thermo-Physical Properties Division at Sandia. Solar absorptance was found using a Beckman 5270 Spectrophotometer. The infrared value was determined using a Gier-Dunkle Infrared Reflectometer.⁶

Using these values, the q''_{is} vs. time profile was calculated. The calculated profile was then used in the HELIOS⁷ computer code at the CRTF to select the heliostats required to achieve the flux levels at time steps which would simulate the environment. The calculated profile and CRTF simulation are shown in Figure 4-2. The pulse shown simulates the first pulse of the string shown in Figure 4-1.

Three differences between the two curves are apparent. First, the CRTF profile is a stepwise simulation of the calculated profile. The calculated profile is simulated by

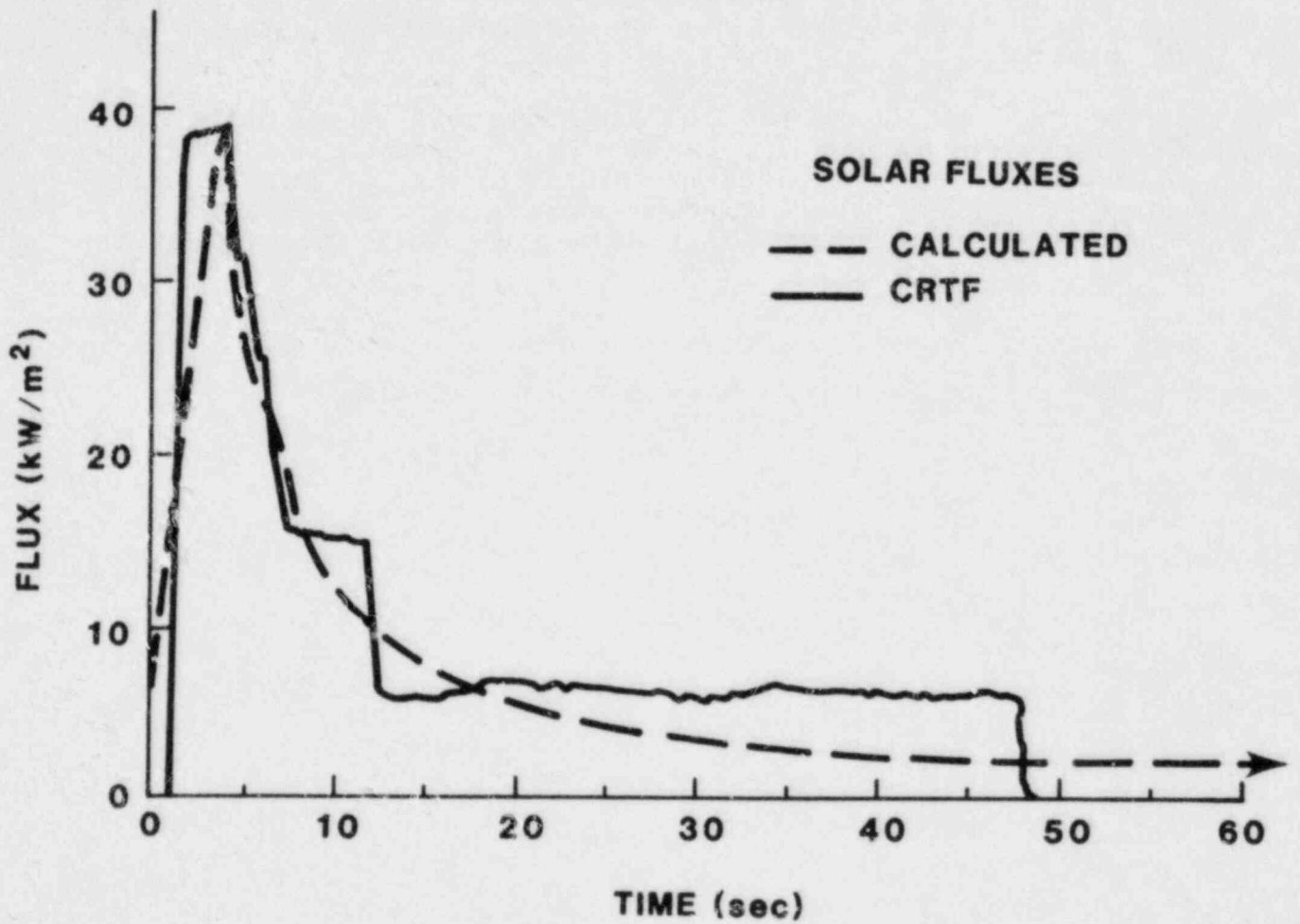


Figure 4-2 Calculated-CRTF Pulse Comparison

starting at the peak calculated flux and removing heliostats individually or in groups to follow the calculated flux decay. This removal produces a step in the flux level. Second, the rapid flux rise of the calculated pulse is simulated by holding the CRTF at peak flux for a short time after opening the shutter and before initiating heliostat removal. This method is used because the time to bring the heliostats onto the target is too long to permit a rapid increase of the flux to the required peak level. Third, the CRTF profile is shorter than the calculated profile. The minimum CRTF flux capability is about 0.5 W/cm^2 (5 kW/m^2), which is three to four times greater than the heat flux in the tail of the calculated profile. Therefore, the CRTF profile is shortened so that the heat content of its tail is equal to the heat content of the tail of the calculated pulse.

A calibration check of the "target" heat flux gauge showed it to be correct to within 4 percent, a good degree of accuracy for the type of heat flux gauge used. During actual component testing, test specimens were mounted adjacent to this gauge and the flux was monitored throughout the test.

5.0 PROFILE AND FACILITY TESTING

The CRTF was confirmed as a simulator of the HECTR-calculated heat flux by comparing the measured temperature rise in an experimental specimen subjected to a CRTF profile with the temperature rise calculated by HECTR for the same specimen.

The flux profile used was that shown in Figure 4-2. This profile simulates the thermal environment in the lower compartment of the Sequoyah containment building due to the first of seven hydrogen burns precipitated by an S₂D event.

The specimen chosen for the comparison was the flat front cover plate from a Barton Model 763 pressure transmitter. This plate was chosen for its simple geometry which simplified the HECTR analysis necessary to calculate its temperature rise. The temperature was monitored by a type K thermocouple imbedded in metalized epoxy in a 6.4 mm (0.250 inch) diameter hole drilled in the back of the plate to within 1.5 mm (0.06 inch) of the front surface of the plate.

Prior to pulse initiation, the plate was heated to temperatures near that calculated by HECTR to be the plate front surface temperature at the start of the first burn using a single heliostat. The specimen was heated approximately 5 K above the starting temperature. The shutter was then closed and the temperature monitored as the remainder of the profile heliostats were focused on the test bay. When the temperature of the plate had drifted back to the desired starting temperature, the shutter was opened and the pulse simulation initiated.

The temperature rises for the CRTF simulation and HECTR calculation were compared with respect to the flux rise and decay portions of the heat flux pulse as well as the pulse as a whole. The results of 24 pulses are summarized in Table 5-1. Results indicate that the desired environment is adequately simulated by the CRTF.

Multiple burns were simulated by the repetition of the pulse used for the single burn simulation. This method is dictated by the combination of two factors: (1) the heliostat control system and (2) natural convection around the test specimen. Because the air in the test bay is cooler than the atmosphere in a containment building under accident conditions, the test specimen will cool faster due to natural convection. The time required to load another profile into the heliostat control computer and bring that profile's heliostats into position would allow the test specimen to cool by convection for an undesirably long time. To obtain the shortest time possible to reposition the heliostats the same pulse was repeated. The pulse having the highest peak

Table 5-1

Comparison of HECTR-Calculated and
CRTF-Produced Temperature Rises

<u>Pulse Region</u>	<u>HECTR</u>	<u>CRTF (24 Pulse Avg)</u>
Flux Rise	4.2/ 7.6	$4.4 \pm 1.0 / 7.9 \pm 1.8$
Flux Decay	8.0/14.4	$8.3 \pm 1.1 / 14.9 \pm 2.0$
Entire Pulse (Rise + Decay)	12.2/22.0	$12.7 \pm 1.3 / 22.8 \pm 2.3$

flux and longest duration (and largest heat content) was used. This pulse was chosen to keep net heat losses (due to convection between pulses) to a minimum over the course of the entire multiple burn simulation. (Results eventually showed that the use of this pulse resulted in a mild degree of conservatism.) The resulting flux profile is shown in Figure 5-1. Slight variations in atmospheric conditions result in slight flux differences from pulse to pulse. The effect is to produce a string of pulses similar to that predicted by HECTR (see Figure 4-1).

Both the HECTR calculation and the CRTF multiple burn simulation showed specimen temperature increasing above the previous peak with each burn. The temperature rises are compared in Figures 5-2a and b. The conservatism introduced by using the pulse with the highest heat content is evidenced by the 64 K (115°F) total temperature rise in the plate produced by the CRTF compared to the 55 K (99°F) rise calculated by HECTR. The entire Barton transmitter casing from which the plate was taken has a mass approximately three times that of the cover plate. Thus, differences in analytically determined and experimentally produced temperatures would not be as great. This being so, the degree of conservatism introduced by repeating the most severe pulse was not deemed great enough to preclude use of the CRTF for multiple burn simulation and testing of the safety related equipment was initiated.

These tests were not designed to be qualification tests; rather, they were exploratory in nature and sought to determine the temperature and operational responses to a strictly thermal environment. As such, the test specimens were not aged nor were they subjected to the preburn LOCA environment or pressure or steam exposure. Thus, any observed changes or degradation in performance would be directly attributable to the simulated hydrogen burn thermal environment.

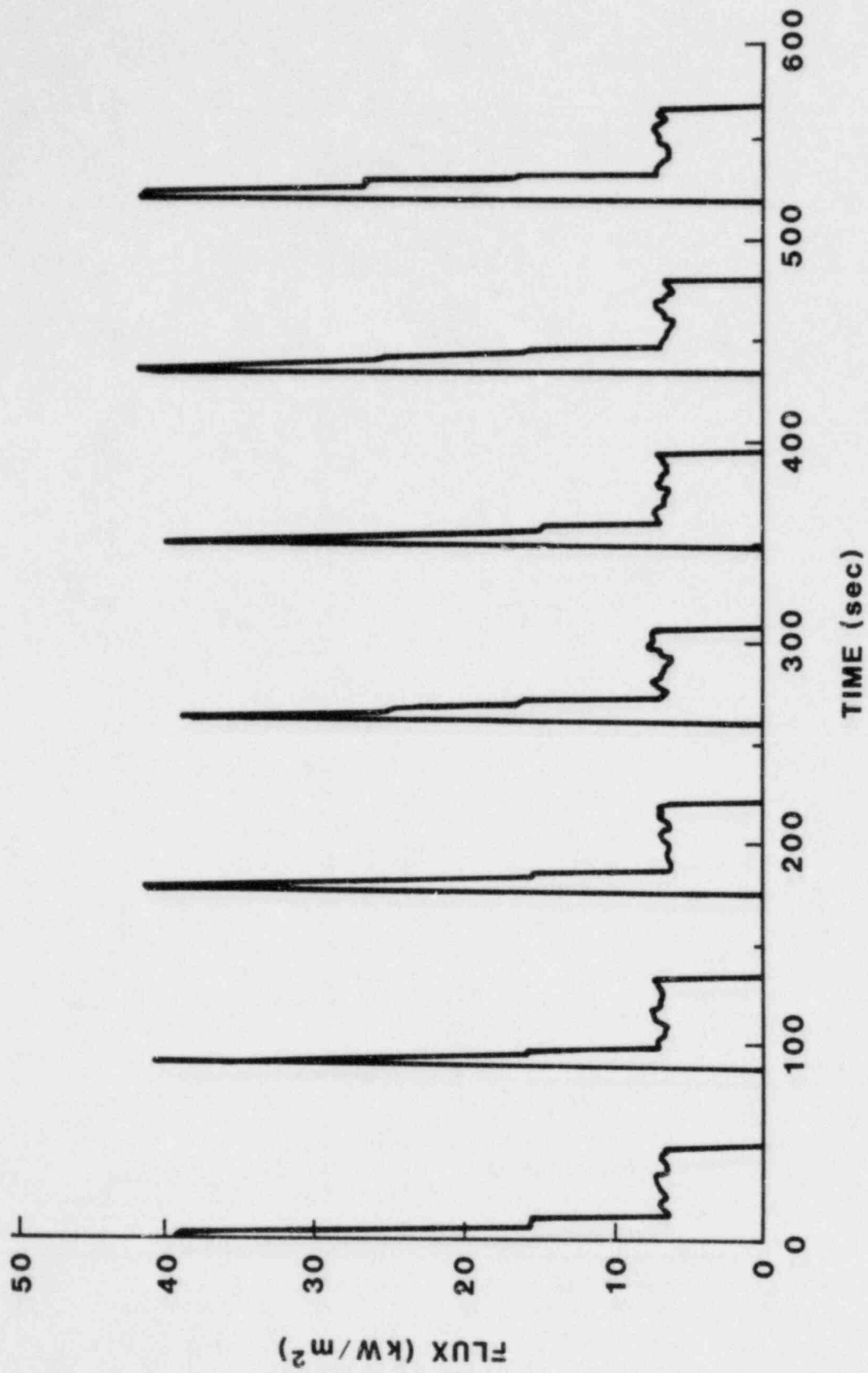


Figure 5-1 CRTF Multiple Burn Simulation

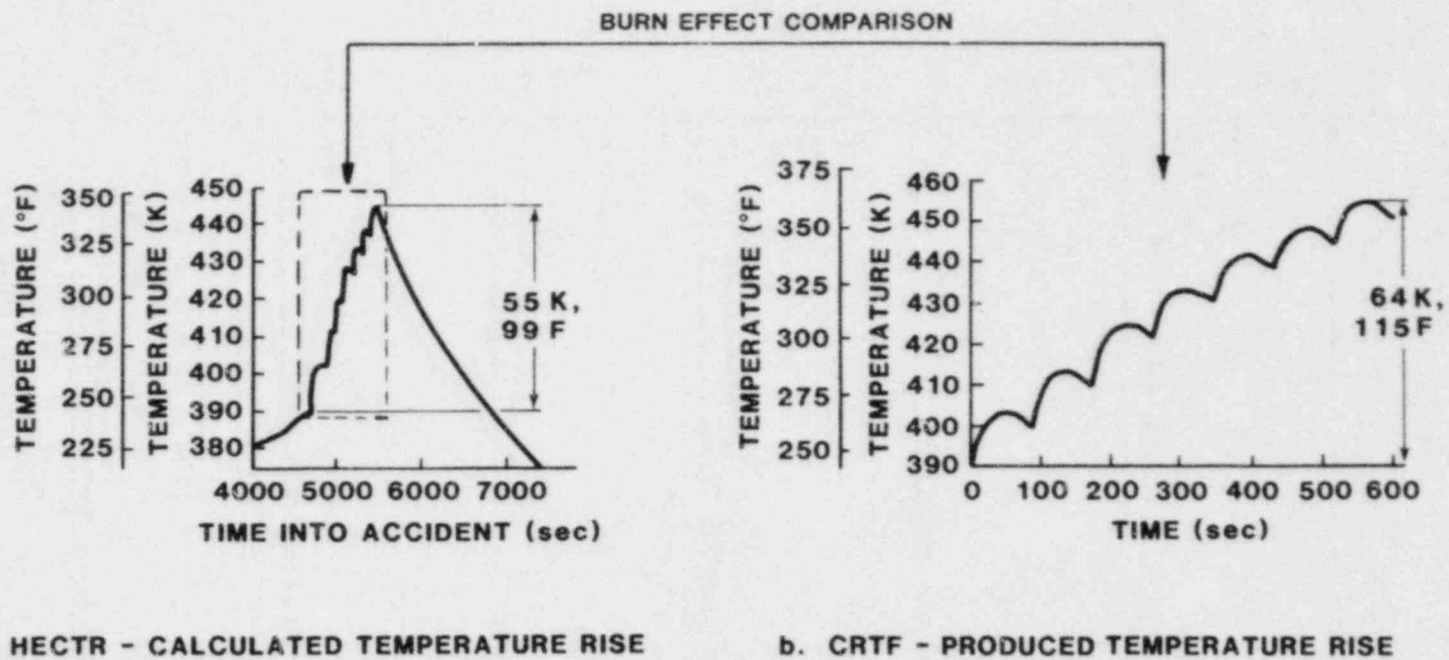


Figure 5-2 Comparison of HECTR-Calculated and CRTF-Produced Temperature Rises for a Multiple Burn

6.0 TEST SPECIMENS, INSTRUMENTATION AND TEST CONFIGURATION

Specimens for the CRTF experiments consisted of seven types of electrical equipment in use in ice condenser containments and throughout the nuclear industry in general. These specimens were:

1. A large gray NEMA-4 electrical enclosure,
2. Two nuclear-qualified terminal blocks,
3. Four cable samples (3 qualified, 1 unqualified),
4. A hydrogen ignitor assembly,
5. Two nuclear-qualified solenoid valves,
6. A nuclear-qualified differential pressure transmitter and,
7. A nuclear-qualified pressure transmitter.

Because the corresponding absorptivities of the painted components were very nearly equal and those of three of the four cables were higher, the CRTF profile shown in Figure 5-1 was used. Prior to profile initiation the specimens were heated to 390 K (242°F). This elevated temperature is representative of exposure to the LOCA environment prior to the first hydrogen ignition.

6.1 NEMA Box

The NEMA-4 box was tested to determine the air temperature inside a large enclosure when subjected to the simulated hydrogen burn environment. The dimensions of the box were 30.5 cm wide x 40.6 cm high x 15.2 cm deep (12 x 16 x 6 inches). The exterior was coated with gray enamel paint. Thermocouples were attached to the inside front door surface and inside surface of the rear wall. A third thermocouple was mounted close to the geometric center of the box to measure interior air temperature.

6.2 Cable and Terminal Blocks

The four cable samples tested were:

1. Thermoelectric WVX, Chromel-Alumel 20 AWG, Type KX, 2 conductors, premium grade, nuclear-qualified,
2. Triangle PWC Inc, WDB, 10 AWG, single conductor, nuclear-qualified,
3. Rockbestos, RSS-6-104, 10 AWG, single conductor, nuclear-qualified and,
4. Generic, RG-58 C/U coaxial, unqualified.

For testing, the cables were mounted and allowed to hang freely between two nuclear qualified terminal blocks. The

terminal blocks were a General Electric EB25A06B6 and a Westinghouse S-542247. Each cable was placed in series with a 500 ohm resistor. A 16 milliampere loop current was maintained during testing. Electrical continuity was monitored during testing and an open circuit between conductors and shields was checked before and after testing.

6.3 Hydrogen Ignitor

The hydrogen ignitor was constructed at Sandia and is similar, in component content and construction, to ignitors used in Interim Distributed Ignition Systems (IDIS) installed in some ice condenser containment buildings. A General Motors Corporation Model GMC-7G diesel glow plug was mounted on the side of a 20.3 cm (8 inch) square by 15.2 cm (6 inch) deep NEMA-4 electrical enclosure. The NEMA box was coated with gray enamel paint. An aluminum spray shield was mounted on the top of the box and a copper heat sink was installed on the glow plug side of the box. Power was supplied to the glow plug by a Dongan Model 52-20-435 multiple tap transformer. The glow plug voltage was 14 V. The assembly is shown in Figure 6-1.

Two temperatures and transformer operation were monitored during the tests. Foil thermocouples were mounted to the inside surface of the enclosure door and on the transformer core. Transformer operation was monitored by connecting the transformer output to a 14 VAC relay. An 8-volt power supply was connected through the relay to a data acquisition channel. This 8-volt signal was monitored throughout the testing. In the event of a transformer failure, the relay would open and the 8-volt signal would be lost.

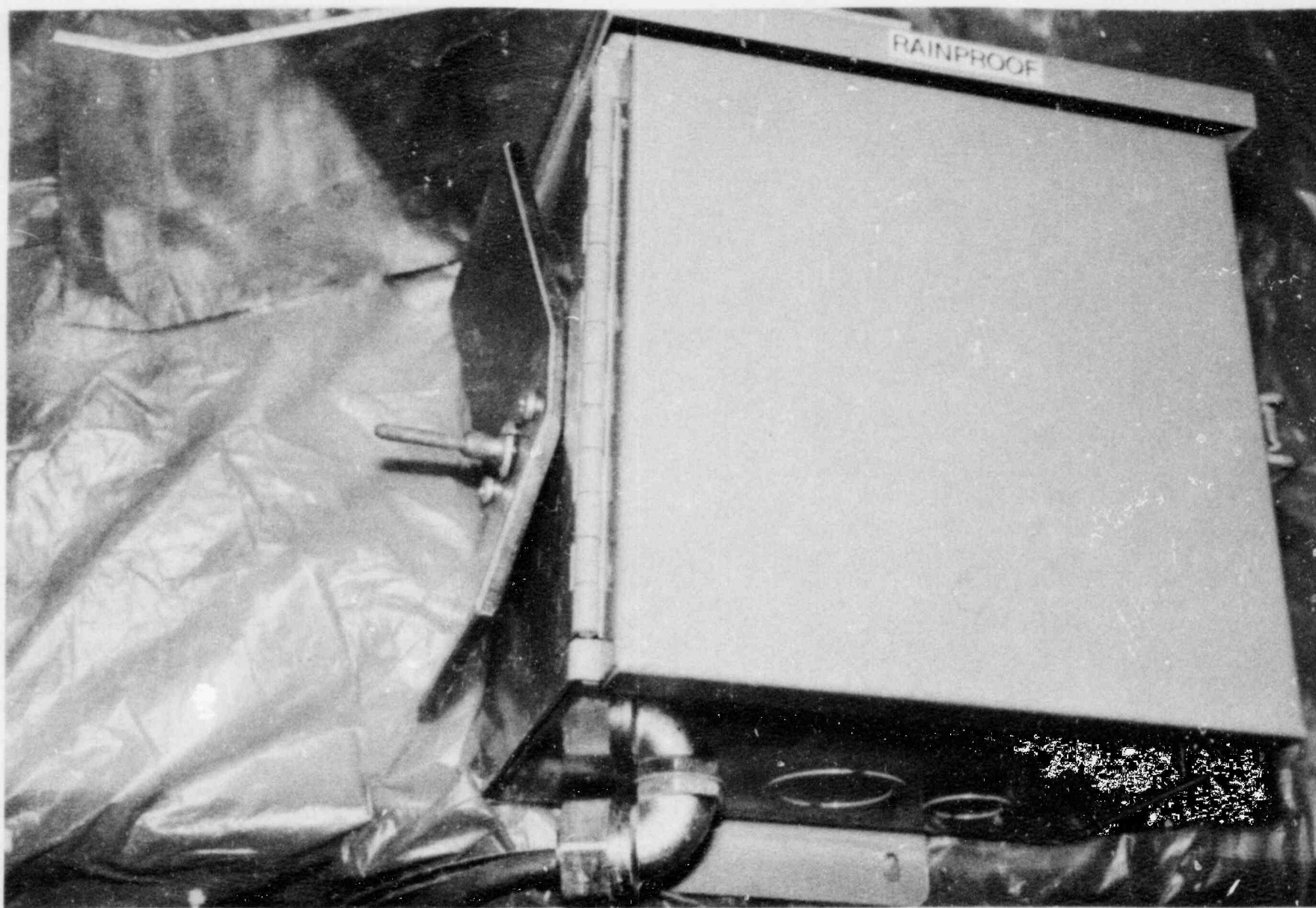


Figure 6-1 Hydrogen Ignitor Assembly

6.4 Solenoid Valves

Two solenoid valves were tested. Both were ASCO Model NP831654E nuclear-qualified valves. One specimen, Serial No. 31457K6, was tested in new condition. It was not previously exposed to any hostile environment. The second valve, Serial No. 31457K10, had undergone several hydrogen burn tests of varying severity at Sandia's Fully Instrumented Test Site (FITS).⁸

Both samples had thermocouples mounted in the top of the solenoid housing and the new valve had an additional thermocouple mounted on the valve body (Figure 6-2).

The test configuration of the valves is shown in Figure 6-3. A source of 120 Vac power was supplied to each valve through a switch operated by a motor-driven timer which activated and deactivated the valve on a 4-second cycle. Valve operation was monitored by a pressure switch mounted to a hose on the output port of the valve. The input port was attached to a nitrogen gas bottle and input pressure was held at 206 kPa (30 psi). This pressure was near the maximum of the system's low-range pressure regulator. An 8 Vdc power supply was connected to a data acquisition channel through the pressure switch attached to the output port hose and a relay. When the valve was activated, the hose on the output port became pressurized, closing the pressure switch. The switch, in turn, closed the relay connecting the 8-volt signal to the data acquisition system. Upon deactivation the hose depressurized, opening the pressure switch and resulting in the loss of the signal.

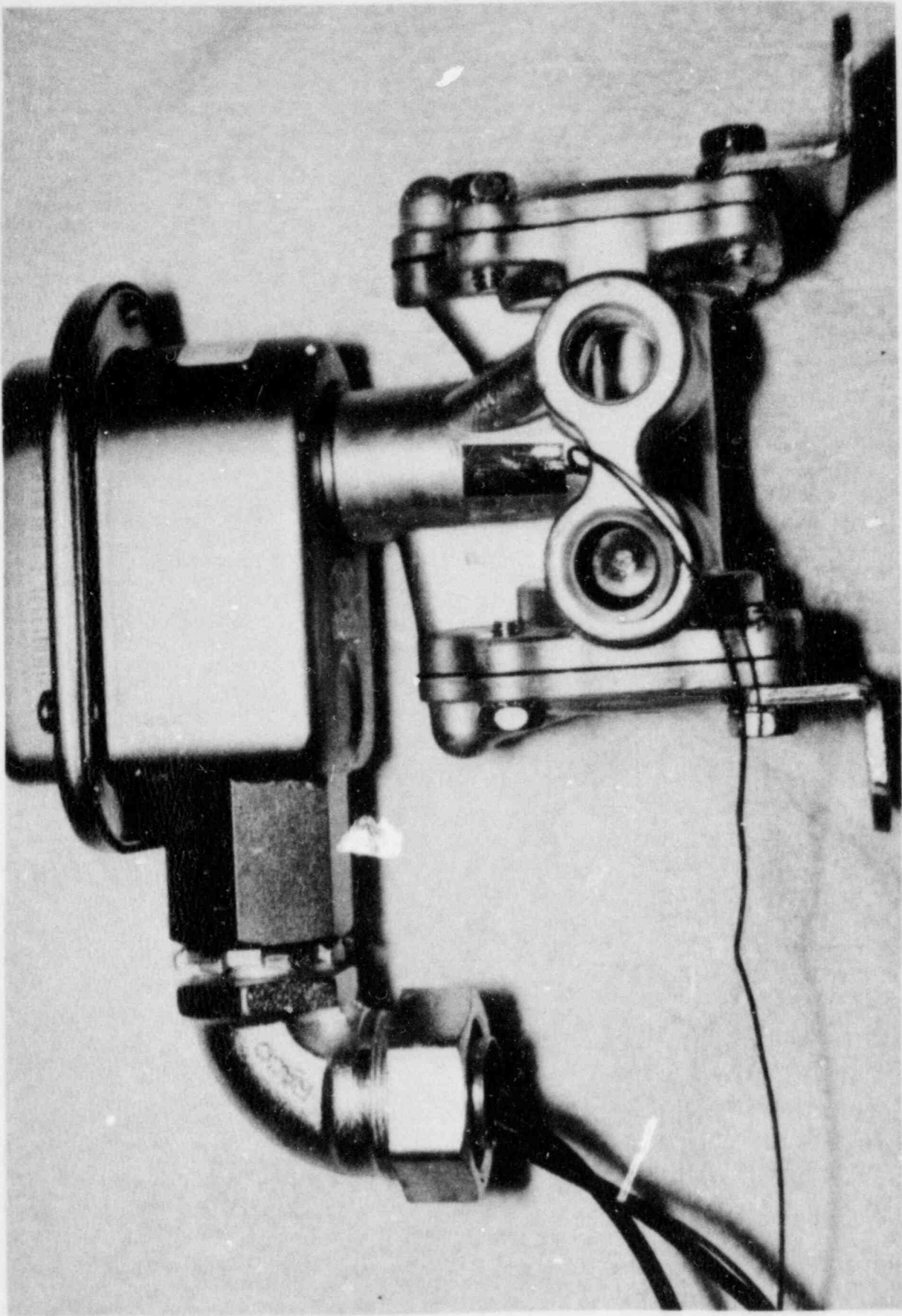


Figure 6-2 New ASCO Solenoid Valve

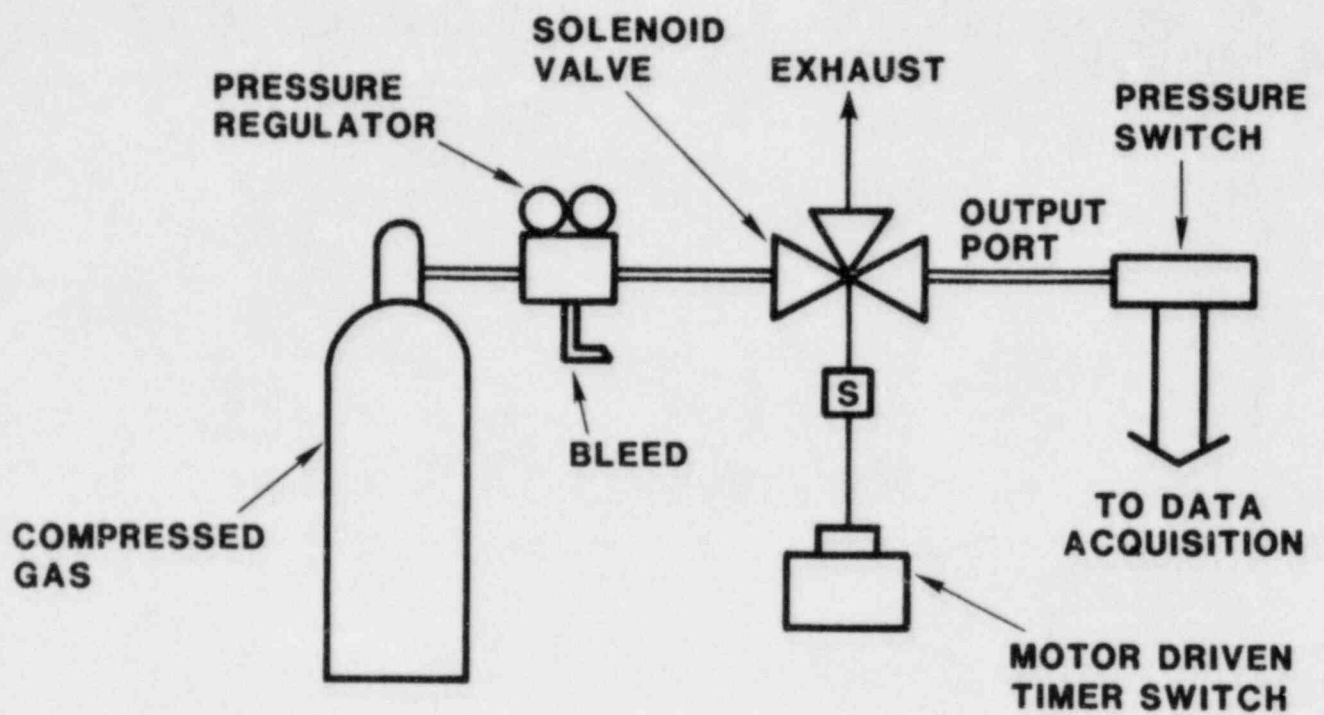


Figure 6-3 Solenoid Valve Function Test Set-Up

6.5 Differential Pressure Transmitter

The differential pressure transmitter tested was a nuclear-qualified Foxboro Model N-E13DM, Serial No. 4695781. Five temperatures were monitored during the testing: the inside surface of the instrument casing, the surface of the amplifier assembly housing, the interior air temperature, the Q2 transistor in the first stage of the DC amplifier and the current amplifier output transistor (Q3). The transistor temperatures were monitored to determine the thermal responses of electrical components inside the amplifier assembly housing. This housing is itself located inside the transmitter casing. Of the two, the current amplifier assembly output transistor passes a larger current and thus operates at a higher temperature.

Also monitored were the amplifier assembly output voltage, force motor output voltage and instrumentation loop current. All are measures of the applied differential pressure and changes in the voltages at constant pressure indicate instrument drift due to thermal effects. The instrument indicates pressure by varying the input power current from 4 to 20 mA, depending on the applied differential pressure. The instrument signal was measured by passing the output current through a 500 ohm (nominal) resistor and measuring the voltage drop across the resistor.

The force motor output voltage rises with decreasing pressure and falls with increasing pressure; i.e., it changes opposite to the instrumentation loop current. This voltage can be as high as 30 volts and because of a 10-volt limitation on the CRTF data acquisition system was divided by 4 using a voltage divider.

The differential pressure limit of the instrument is 50 kPa (7.2 psi) and during testing differential pressure was maintained at 48.3 kPa (7 psi). This pressure was chosen so that instrument electronics would be operating at near maximum current during testing.

The instrument, as tested, is shown in Figure 6-4. The test set up is shown in Figure 6-5.

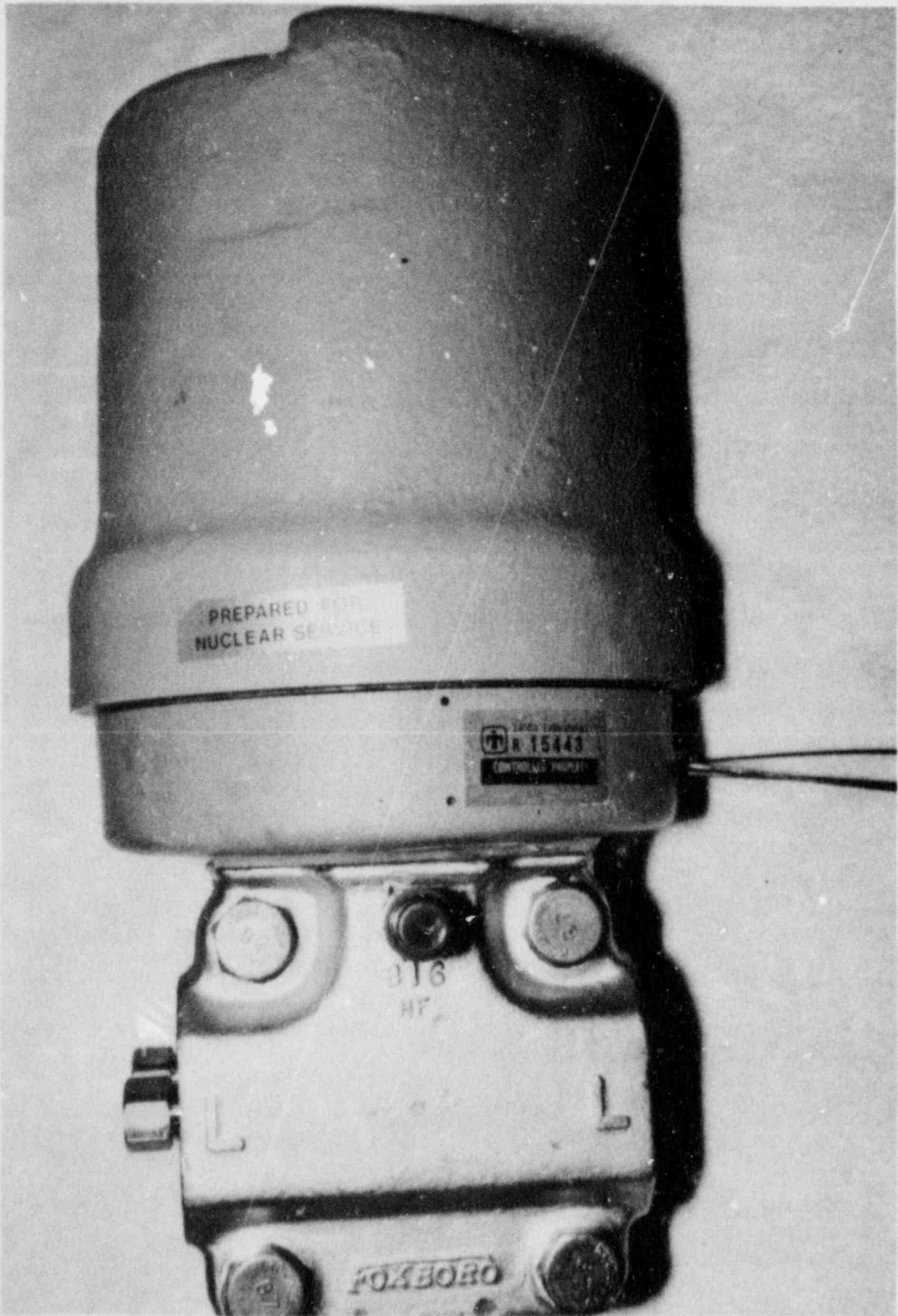


Figure 6-4 Foxboro Differential Pressure Transmitter

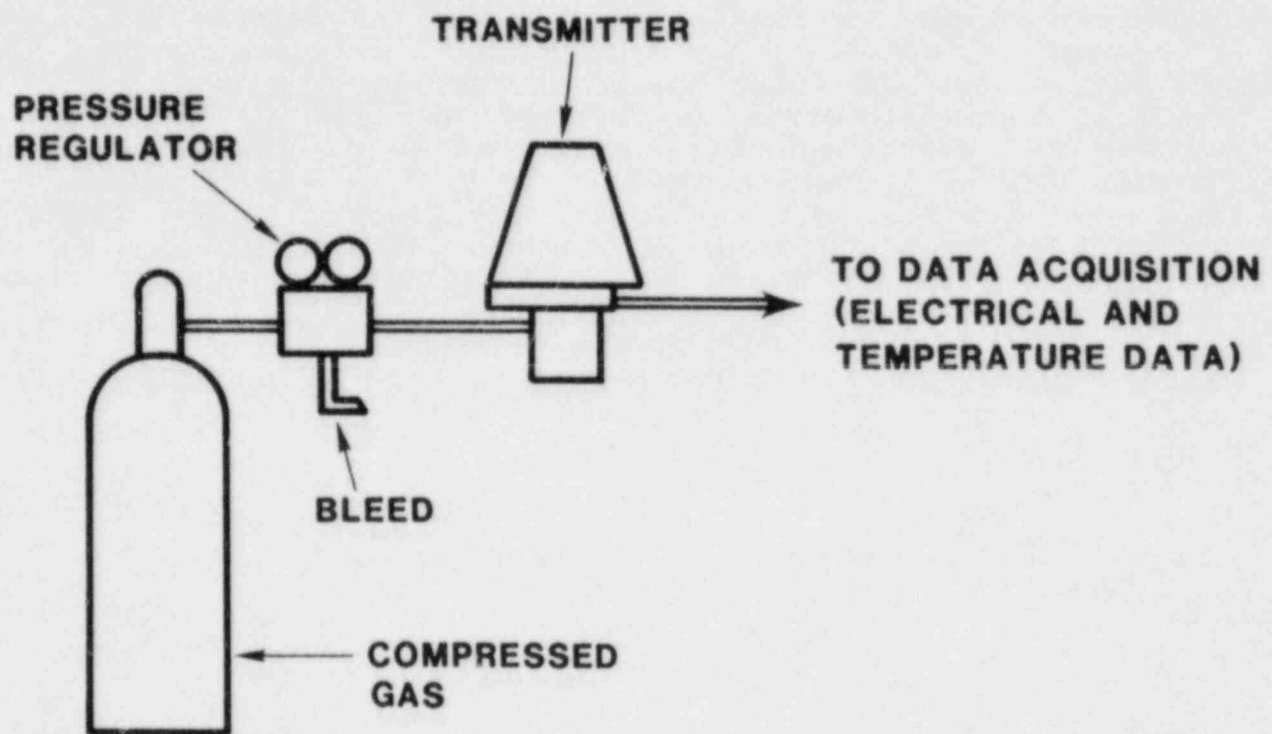


Figure 6-5 Transmitter Test Set-Up

6.6 Pressure Transmitter

The pressure transmitter tested was a Barton Model 763, Serial No. 1126. Seven temperatures were monitored. The temperature of the front face of the instrument was taken to be that measured by a thermocouple imbedded in a blind hole drilled from the rear surface of the front cover plate to within 1.5 mm (.06 inch) of the front surface. Other casing temperatures measured were the rear surface of the front cover plate and the rear of the instrument casing. The interior air temperature was also monitored. Electronic component temperatures monitored were that of the noise suppression capacitor, a relatively massive component, the voltage regulator pass transistor and one of the current amplifier output transistors. Temperatures of these electronic components were measured for the same reason as discussed in Section 6.5 for the Foxboro instrument. Four electrical signals were also monitored: the voltage reference power supply voltage, the current amplifier voltage, the operational amplifier output voltage and the instrument signal. The instrument loop current measured in the same manner as described in Section 6.5 for the Foxboro transmitter. The overall test set up for the Barton instrument was also similar to that for the Foxboro transmitter. During testing the instrument was pressurized to 15.5 MPa (2250 psi), a typical value for a PWR primary coolant loop.

The instrument is shown in Figure 6-6.

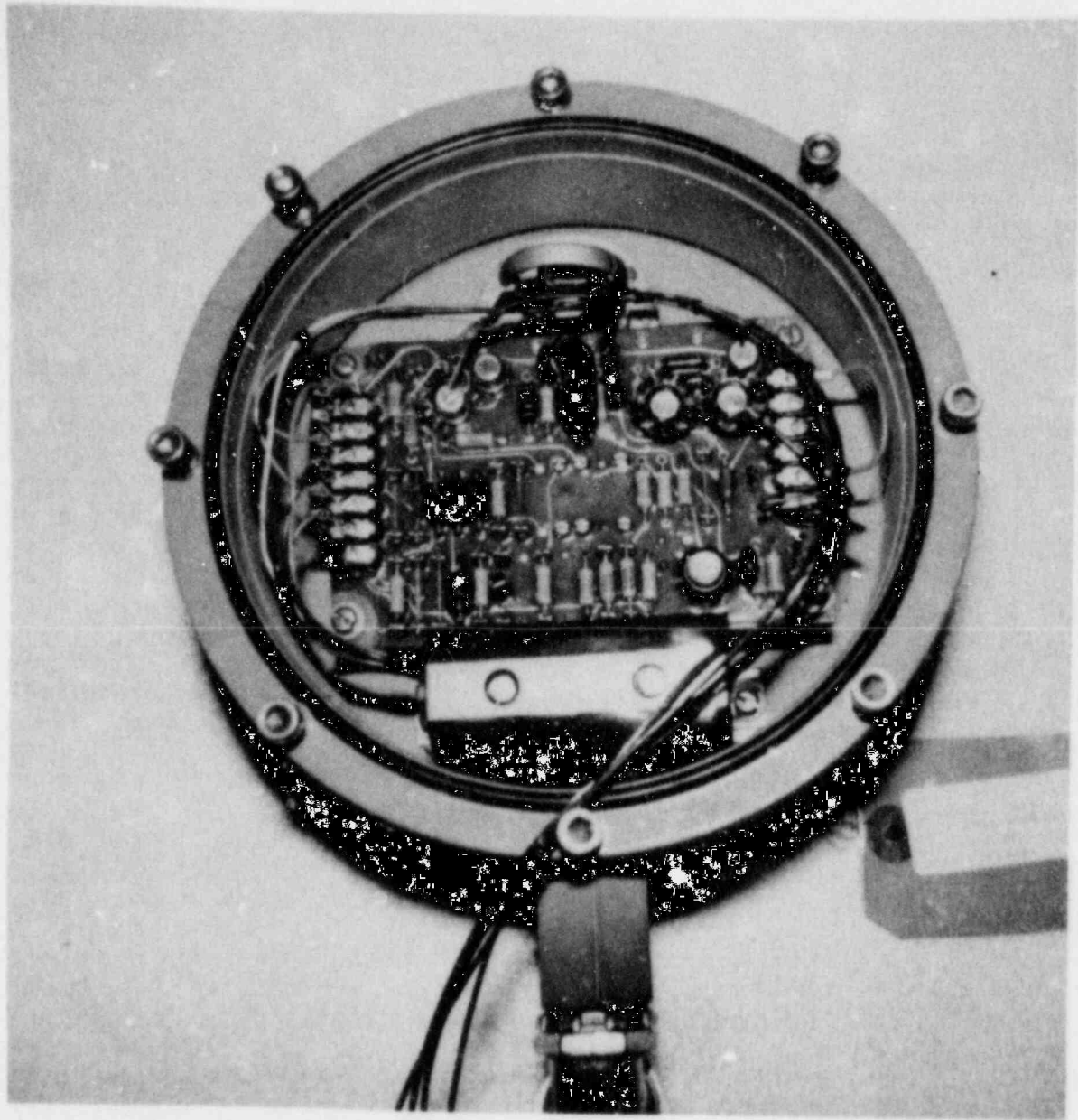


Figure 6-6 Barton Pressure Transmitter

7.0 TEST PROCEDURE

The test procedure consisted of three basic steps:

1. Activate test specimens
2. Preheat test specimens to the preburn temperature predicted by HECTR
3. Expose the specimens to the multiple burn simulation.

Activation of the specimens was quite simple. It involved attachment of appropriate hoses and closing of electrical circuits providing power to the various samples.

The multiple burn simulation was accomplished using the same procedure and flux profile described in Section 5.0. After the completion of the first pulse the shutter closed automatically and heliostats were repositioned on the shutter. The shutter was again opened and the specimens were again exposed to the same pulse. This sequence was repeated until the test items had been exposed to the seven pulses.

Preheating of the test specimens was somewhat different than for the flat cover plate used in the facility characterization. In the scenario considered, the first hydrogen burn does not occur until over an hour into the accident. During this time, equipment in the lower compartment would be exposed to the high temperature LOCA environment produced by steam released during the accident. This high temperature steam bath causes the equipment to slowly rise to a temperature of about 390 K (242°F). The slow rise results in reasonably uniform temperature distributions in individual pieces of equipment. Slight gradients may be present if the components are mounted to a heat sink such as the containment wall. Therefore, to simulate the hydrogen burn thermal environment as closely as possible, it was necessary to preheat the specimens in a manner that would minimize temperature gradients in them. To accomplish this the test items were preheated in stages using a single heliostat to minimize heat flux. The temperature just behind the front facing surface of the test item was monitored. The shutter was opened exposing the test specimen to the solar flux from a single heliostat. The monitored temperature was allowed to rise to about 397 K (255°F). At this temperature the shutter was closed and the specimen front was allowed to cool to about 390 K (242°F). During this cooling, heat was transferred by conduction from the heated front surface of the component to the cooler sides and rear surfaces. When the monitored temperature had fallen to 390 K the heating was repeated. The minimum temperature gradient was achieved when the time for the monitored temperature to drift from

397 K to 390 K was roughly the same on two successive exposures. The specimen was then heated to 397 K one more time, the shutter was closed and while the temperature drifted back to 390 K for the last time the full complement of heliostats necessary for the hydrogen burn simulation was focused on the shutter. When the monitored temperature reached 390 K the shutter was opened and the burn simulation was initiated.

8.0 RESULTS

8.1 NEMA Box

The large NEMA box was tested simultaneously with the ignitor assembly and new solenoid valve. The front door of the ignitor assembly front door was monitored for the 390 K starting temperature. Because a portion of the NEMA box was in a somewhat cooler part of the preheat beam its starting temperature was somewhat lower, 369 K (204°F). Results are shown in Figure 8-1.

The NEMA box front door exhibited distinct stepwise temperature increases through the test rising to a maximum temperature of 475 K (395°F). The back temperature rose nearly linearly with time from 320 K (116°F) to 331 K (195°F). The air temperature inside the box shows very slight increases with each pulse application as it rose in temperature from 331 K (137°F) to a maximum of 391 K (245°F). These results are summarized in Table 8-1. T_i is the temperature at the start of the first pulse; T_f is the final peak temperature (at the end of the final pulse).

Table 8-1

NEMA Box Temperature Rises

<u>Region</u>	T_i (K/°F)	T_f (K/°F)	ΔT (K/°F)
Front Door	369/204	475/395	106/191
Back	320/116	364/195	44/ 79
Interior Air	331/137	391/245	60/108

8.2 Terminal Blocks and Cable

The small diameter of the cable specimens and the surface characteristics of both the cables and terminal blocks prevented attachment of thermocouples to these samples. Because of this and because of the low thermal masses and low thermal conductivities of the samples which would have lead to rapid cooling between preheating and the burn simulation the samples were not preheated.

Exposure to the simulated hydrogen burn produced no severe adverse effects on any of the cable samples or terminal blocks. The cables and terminal blocks were exposed to a total of six multiple burn simulations and were visually inspected between tests. Due to a sudden reduction in insolation (the amount of available solar energy at the Earth's surface) the flux levels of the first two simulations were

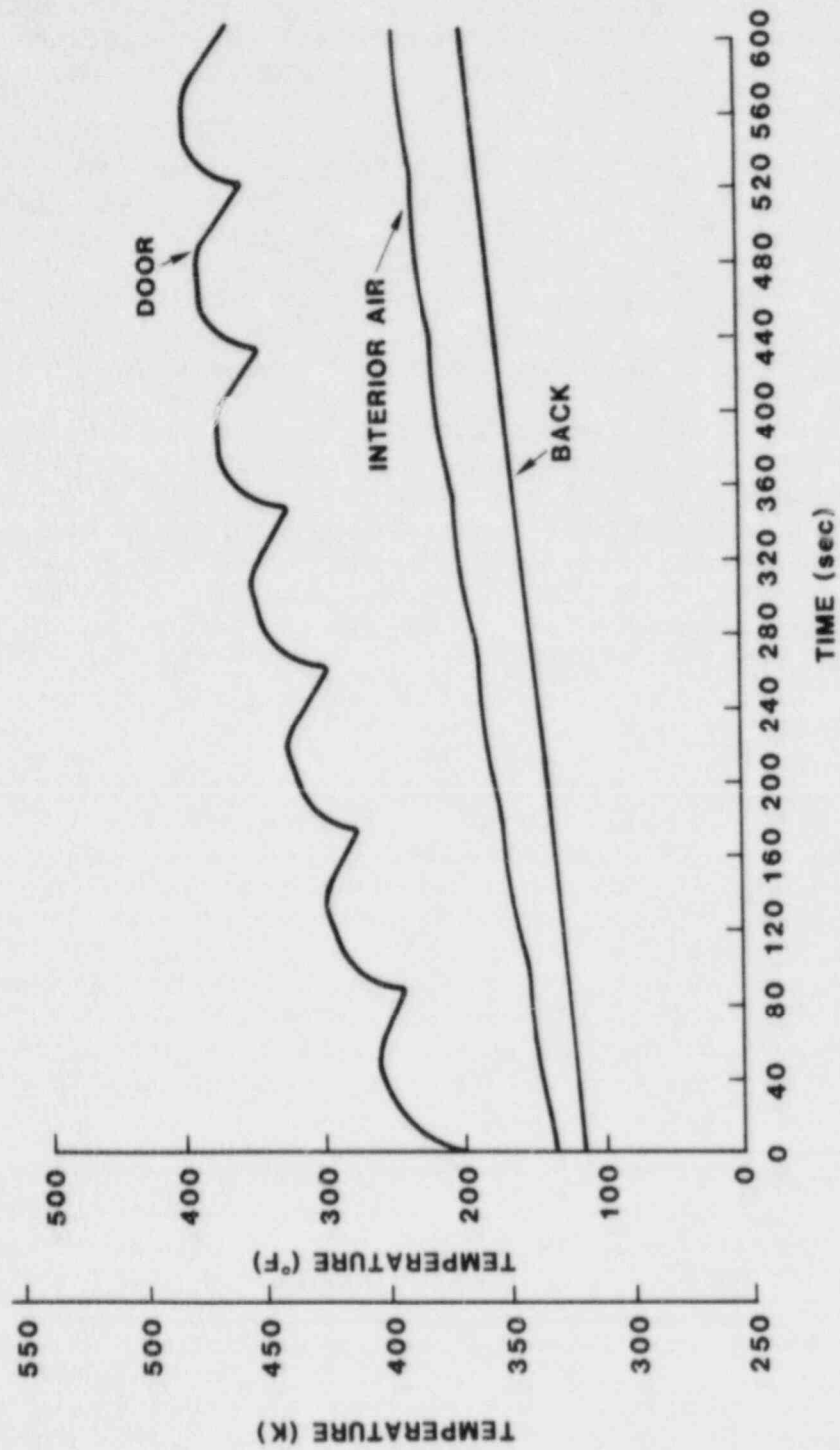


Figure 8-1 NEMA Box Temperatures

about 10 percent low. During these tests the cables maintained electrical continuity with no fluctuation in the loop current. Visual inspection found no physical damage to any of the samples. A thin plastic cover over the Westinghouse terminal block melted after the first simulation. This was expected and it in no way affected the function or appearance of the terminal block. Subsequent simulations were conducted at full flux levels.

The first simulation at full flux level produced a small blister, roughly 3 mm by 6 mm (0.125 x 0.25 inch), at the mid-point of the unqualified RG-58 cable sample. A slight amount of insulation melting was also evident at the ends of the same cable where it was attached to the terminal blocks. Again all cables functioned properly. Aside from the RG-58 sample no other physical effects were evident.

Exposure to two more simulations did not affect cable or terminal block performance. All samples maintained electrical continuity and no further degradation in the jacket of the unqualified RG-58 sample was found. After the fifth simulation some material browning was noted on the white fabric jacket of the Thermoelectric nuclear qualified cable. No further darkening could be detected after the sixth and final exposure.

8.3 Hydrogen Ignitor

The hydrogen ignitor assembly was subjected to four simulations. Results shown in Figure 8-2 are typical of all four. Because of the low heat capacity of the enclosure it cooled to 386 K (235°F) prior to the simulation. Since the enclosure was of the same construction as the large NEMA box previously described, it is logical that the temperature response should also be the same. Figure 8-2 shows this to be so. The temperature of the assembly door increases from 386 K to a maximum of 491 K (424°F), exceeding the LOCA qualification by 47 K (85°F) (assuming a qualification temperature of 444 K, 340°F).

The massive core of the transformer exhibits no such behavior. Starting from a preheated temperature of 371 K (209°F) the temperature rises at a reasonably constant rate to 385 K (234°F).

Throughout the testing the transformer output remained constant at approximately 14 volts. The assembly was visually inspected between simulations to check operation of the glow plug. It is not surprising that the glow plug continued to function since the diesel engine environment for which it is designed is much more severe than the hydrogen burn environment.

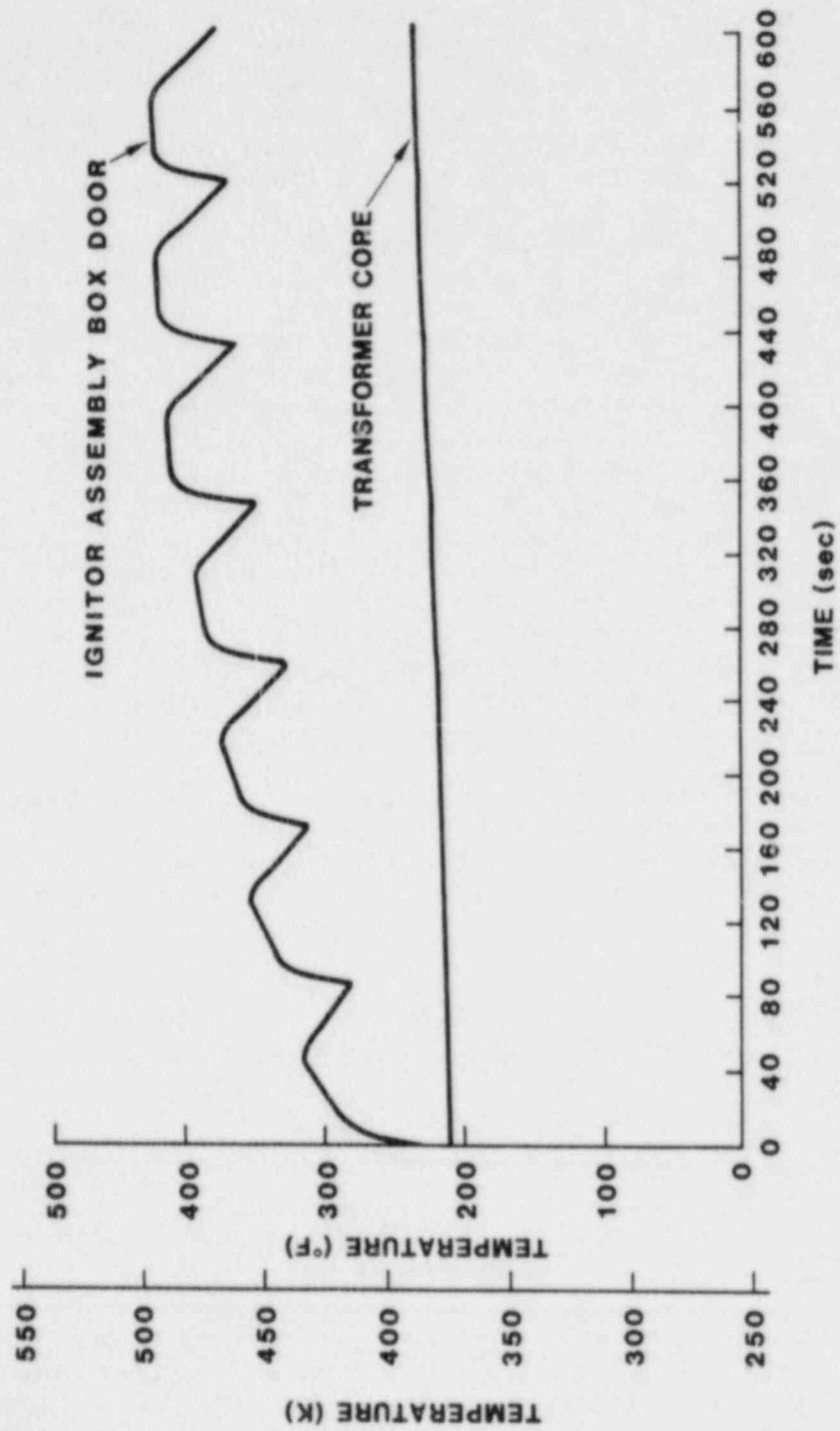


Figure 8-2 Hydrogen Ignitor Temperatures

8.4 Solenoid Valves

The first valve tested was the one in new condition. The valve was subjected to four simulations and operated normally throughout the testing. A portion of the signal from the pressure switch which monitored valve operation is shown in Figure 8-3. The 8-volt signal indicates that the solenoid has been activated and the valve has opened pressurizing the hose on the outlet port. The zero volt signal indicates that the solenoid has been deactivated closing the valve and exhausting the pressurized hose. This cycle was repeated approximately every four seconds throughout the testing. Each test involved approximately 150 cycles.

For preheating purposes the temperature of the hydrogen ignitor front door was monitored. When this temperature reached 390 K the simulation was initiated. The temperature responses of the solenoid housing and the valve body are shown in Figure 8-4. As with other sheet metal specimens, the solenoid housing exhibits distinct temperature ratcheting. Starting from a temperature of 353 K (176°F) the housing reached a maximum temperature of 416 K (289°F) during the sixth pulse and returned to 415 K (287°F) during the seventh and final pulse. This may indicate the attainment of some degree of equilibrium. Similar, nearly identical, results were obtained from the final test. Results are shown in Figure 8-5. Starting at 355 K (179°F) the solenoid rises to 416.9K (291°F) in the sixth pulse and is only slightly warmer at 417 K (292°F) at its maximum temperature in the final pulse.

The brass valve body exhibits a small degree of temperature increase with each pulse in rising from 321 K (119°F) at the start of the test to a final temperature of 341 K (154°F). These results are summarized in Table 8-2.

Table 8-2

New Solenoid Valve Temperature Responses

Valve Component	T_i (K/°F)	T_f (K/°F)	ΔT (K/°F)
Solenoid Housing	353/176	415/289	62/113
Valve Body	321/119	341/154	20/ 35

The low starting temperatures and relatively small temperature rises are due to the high degree of reflectance of the solenoid housing and valve body. The solenoid housing is fabricated from stamped metal with an unpainted shiny surface and the valve body is made from brass and also

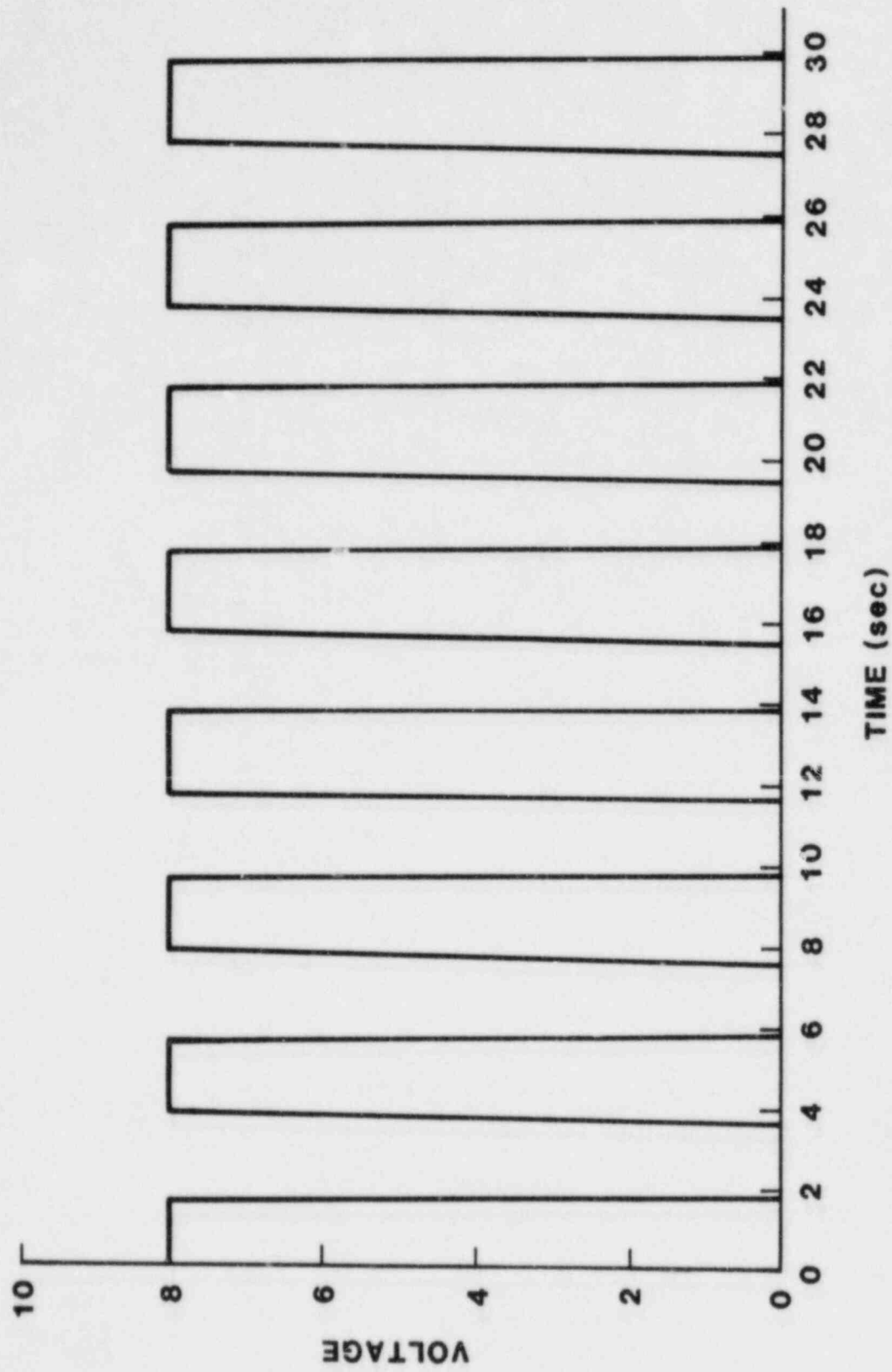


Figure 8-3 Solenoid Valve Operation Signal

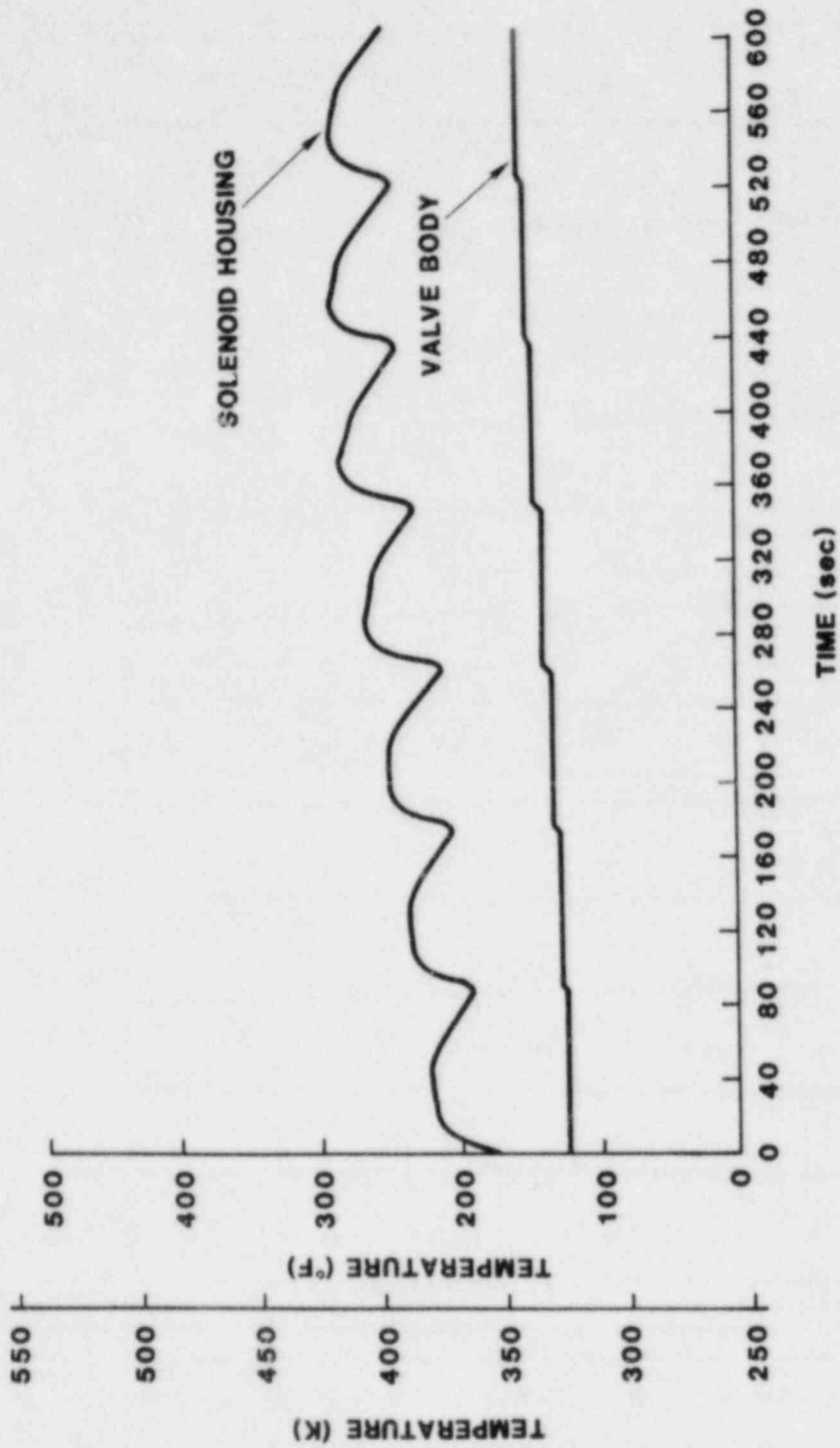


Figure 8-4 New Solenoid Valve Temperatures (First Test)

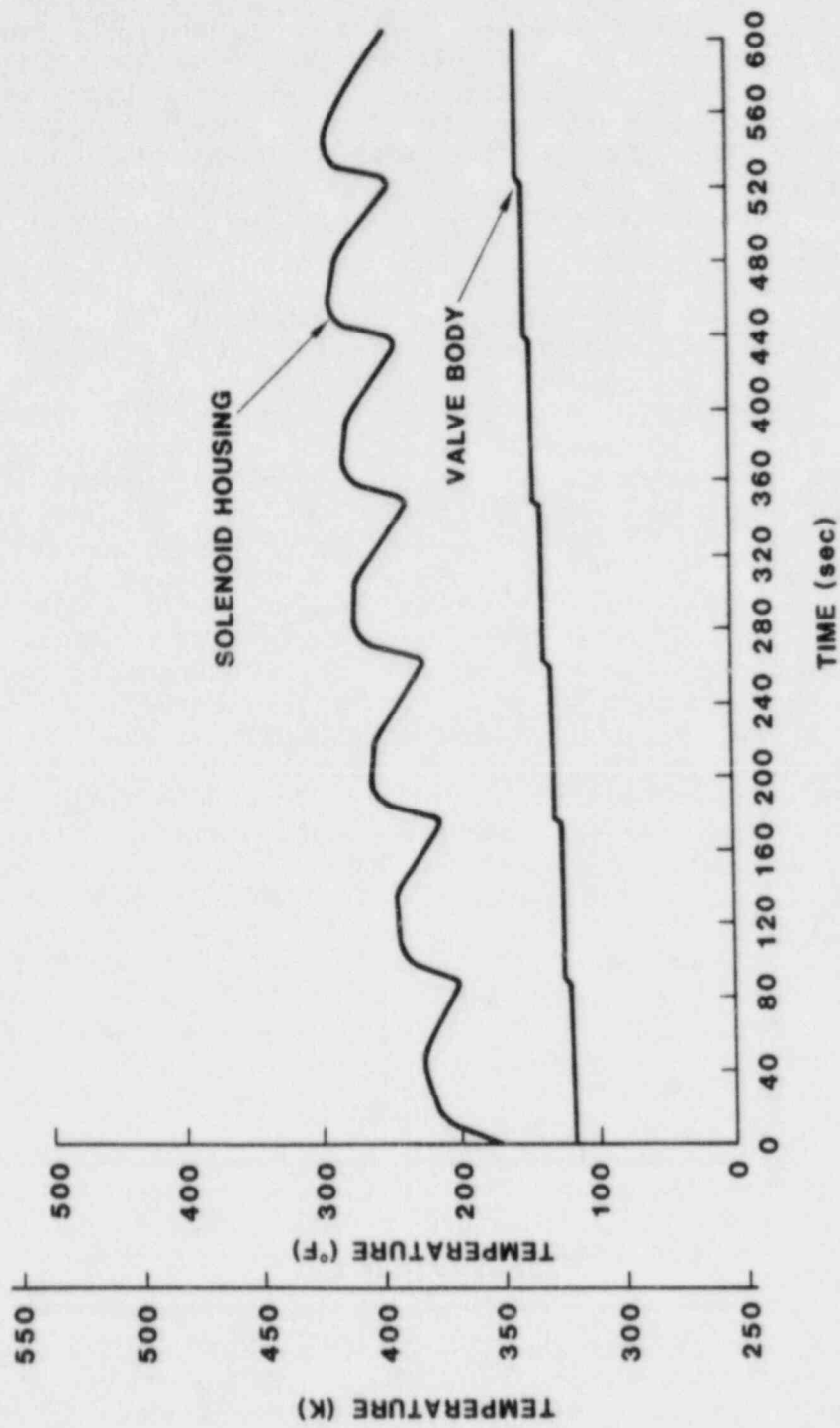


Figure 8-5 Final New Valve Temperatures (Fourth Test)

uncoated. Thus, despite the low thermal masses of the two valve components, both exhibit relatively mild thermal responses to the imposed environment.

Results from the testing of the previously tested valve (FITS valve) were inconclusive. Winds blowing directly on the sample during testing resulted in small temperature rises. This is shown in Figure 8-6. The starting temperature was 329 K (133°F) rising to 351 K (172°F). When the valve was tested at the FITS facility only the solenoid housing temperature was monitored and no thermocouples were added for the CRTF testing. Therefore, no valve body temperature data is available.

Valve operation was monitored throughout testing. As with the new valve, the FITS valve functioned normally.

8.5 Foxboro Differential Pressure Transmitter

The Foxboro transmitter is a very massive object. The sample considered in the present series of tests was equipped with a cast iron case and had a mass of approximately 19 kg (42 lb).⁹ This large mass required nearly 20 minutes to achieve the starting temperature of 390 K on the inside surface of the case. Such slow heating results in minimum temperature gradients throughout the specimen and very closely simulates the gradual heating produced by the preburn LOCA environment. This slow initial heating also indicates that the temperature rise during the burn simulation should be low. This is borne out by the results shown in Figure 8-7. The casing shows a higher temperature with each successive burn, but not to the degree exhibited by components of lower thermal mass described in earlier sections of this report. Also apparent is a slight delay between the initial flux exposure and the start of the temperature rise on the inside surface of the casing and the interior air. This is due to the considerable mass of the transmitter and the thickness (0.5 inch, 12.5 mm) of the casing. Starting from 390 K (242°F) the casing inside surface reaches a maximum of 398 K (257°F). The interior air temperature follows the casing temperature rising from 377 K (219°F) to 386 K (236°F). The amplifier assembly housing rises steadily from 366 K (200°F) to 376 K (218°F). Temperatures of the two monitored transistors are given in Figure 8-8. Both are located inside the amplifier assembly housing and exhibit gradually rising temperature. The Q2 transistor rises from 359 K (187°F) to 369 K (205°F). The amplifier output transistor carries a larger current than the Q2 and thus operates at a higher temperature. It rises from 366 K (200°F) to 376 K (218°F). Temperature rises are summarized in Table 8-3.

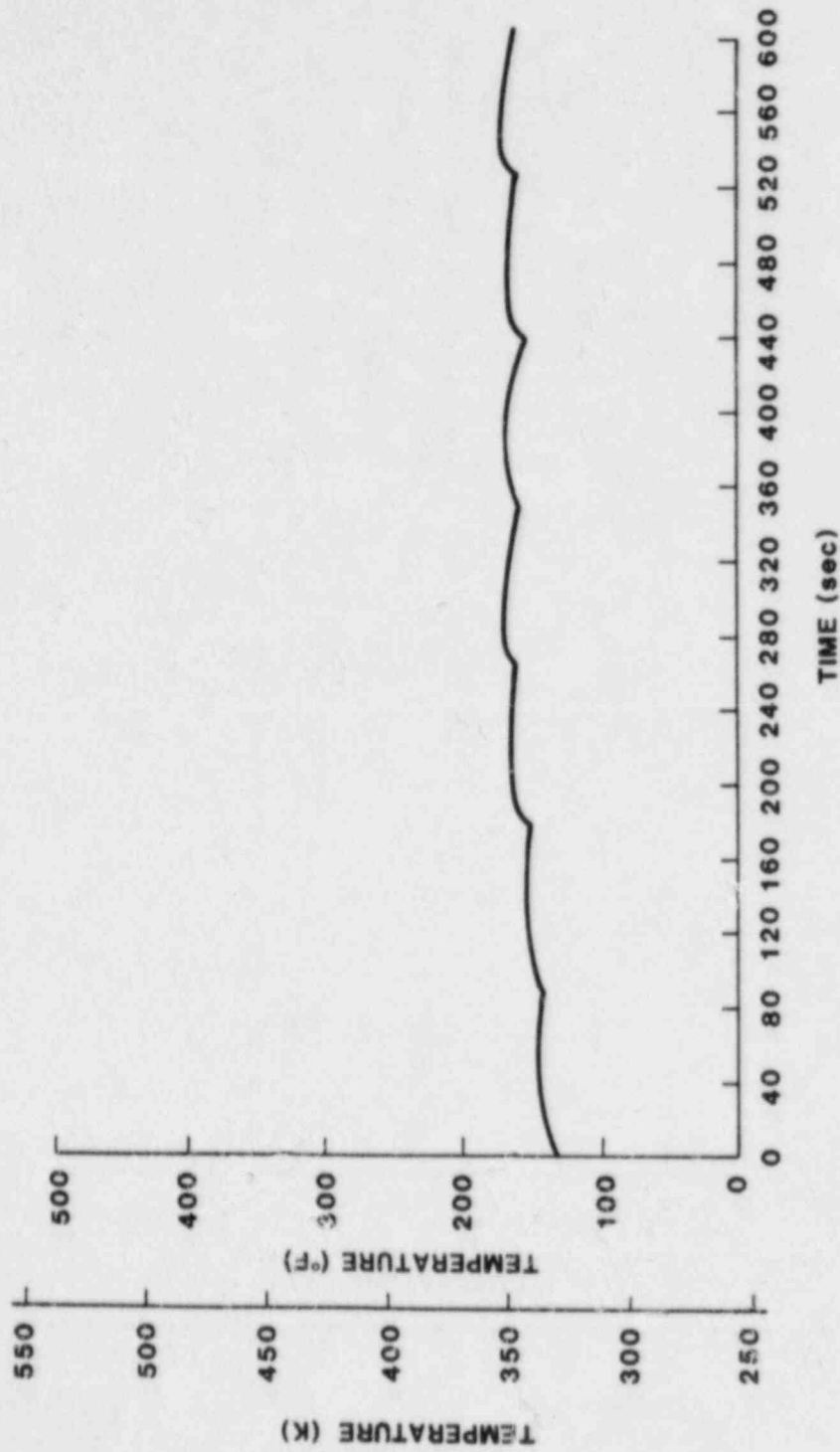


Figure 8-6 FITS Valve Solenoid Housing Temperature Response

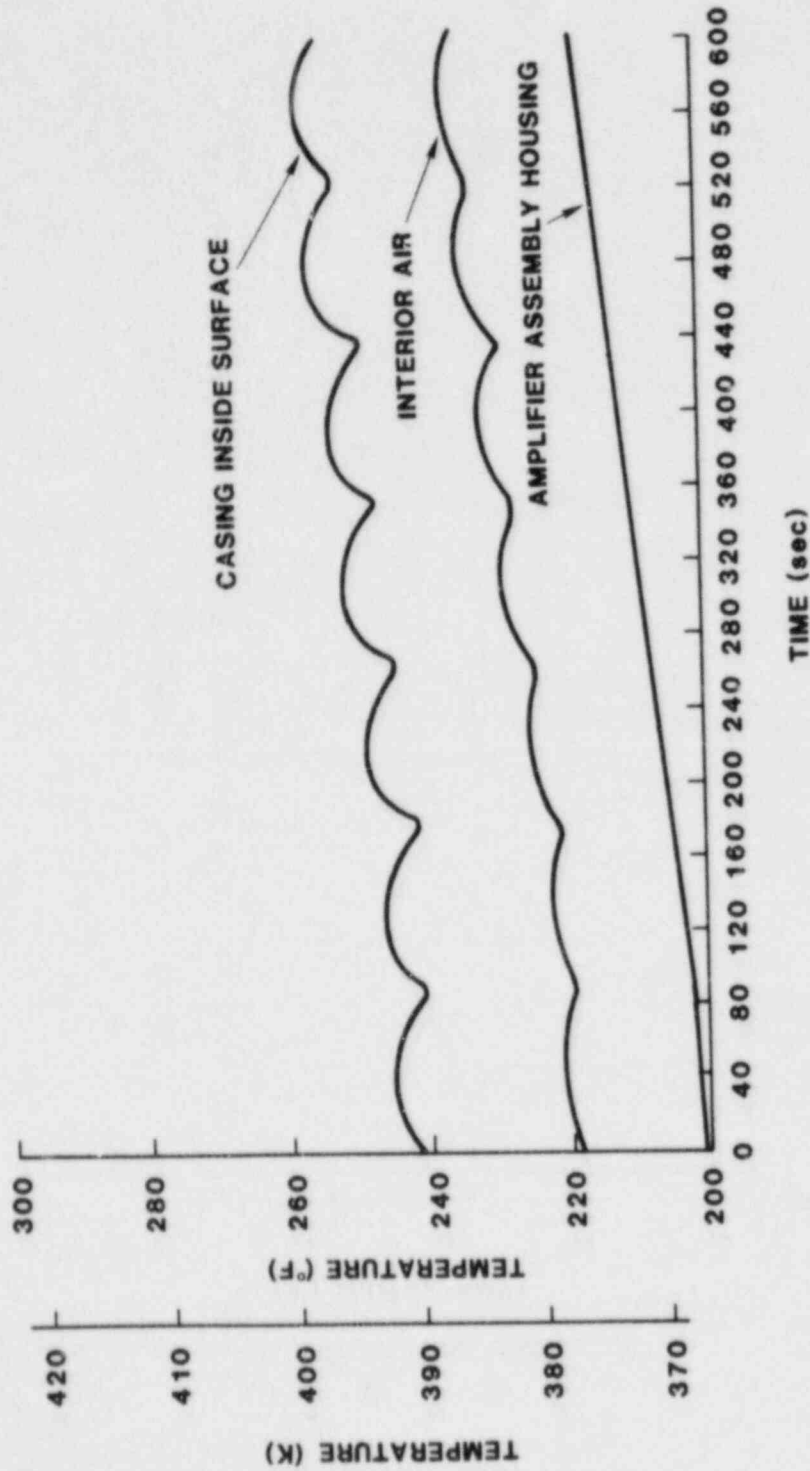


Figure 8-7 Foxboro Transmitter Temperature Responses
(Non-Electronic Components)

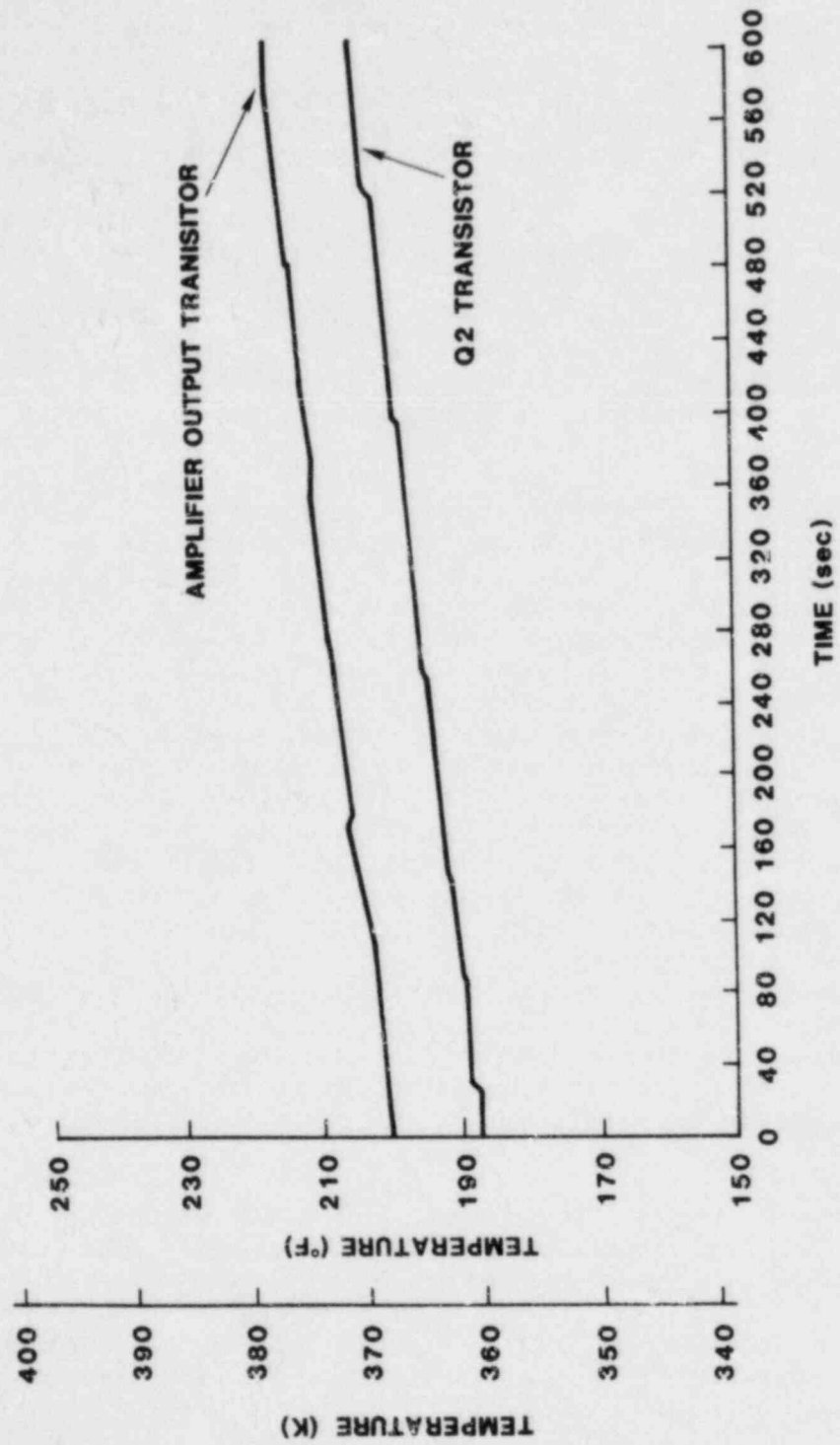


Figure 8-8 Foxboro Transistor Temperature Responses

Table 8-3

Foxboro Transmitter Temperature Rises

Valve Component	T_i (K/°F)	T_f (K/°F)	ΔT (K/°F)
Casing Inside Surface	390/242	398/257	8/15
Interior Air	377/219	386/236	9/17
Amp Assembly Housing	366/200	376/218	10/18
Q2 Transistor	359/187	359/205	10/18
Amplifier Output Transistor	366/200	376/218	10/18

During testing, a differential pressure of 48.3 kPa (7 psi) was maintained across the instrument. This value is close to the 50 kPa (7.3 psi) limit of the device. Instrument performance is shown in Figure 8-9. The amplifier assembly input voltage remains constant as expected at about 0.75 volts. Slight fluctuations are apparent in the force motor voltage and instrument signal. Rises of 0.075 volt in the instrument signal indicating a small pressure rise of 0.48 kPa (0.07 psi) are accompanied by a drop in force motor voltage as expected. Initially it was suspected that these fluctuations indicated some malfunctions in the transmitter. The periodicity of the fluctuations ruled out random variations in the pressure regulator. However, in the interests of thoroughness, the regulator was checked and found to be working properly. A set of data was taken immediately after the fluctuations were noticed and while the transmitter was still at elevated temperature but without exposure to heliostats. Prior to testing the instrument had been checked out and no signal fluctuation was evident. Nor was any fluctuation found in this data scan immediately following the test.

The instrument signal was then compared with the heat flux measurements. It was found that the signals indicating the pressure rise corresponded exactly with exposure to the heat pulse. The experiment set up in the tower test bay was then examined. It was determined that the hose supplying pressure to the transmitter, though insulated, was experiencing some heating during exposure to the concentrated solar flux. This caused a slight increase in the pressure of the nitrogen inside the hose which the instrument detected. Upon termination of the pulse the hose, having a small heat

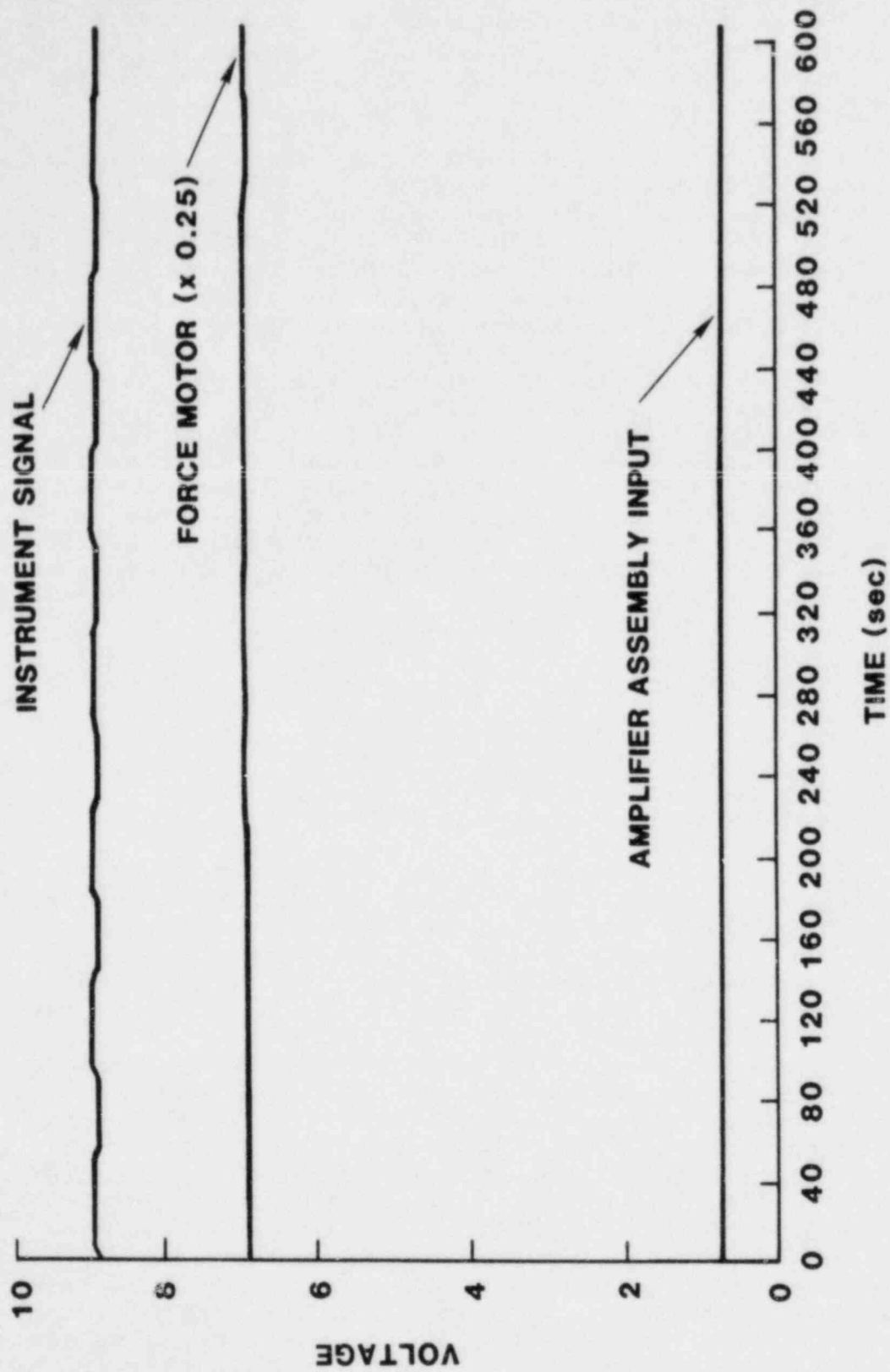


Figure 8-9 Foxboro Transmitter Performance

capacity, quickly cooled to its original state and the pressure returned to the regulator set point. So, the signal fluctuation was not an instrument malfunction but rather a response to a slight change in experimental conditions.

The Foxboro N-E13DM differential pressure transmitter performed generally as it was designed to in that it produced a constant signal at a constant applied differential pressure (disregarding the fluctuations due to heating of the pressure hose). There were, however, some changes in performance that became evident only after exposure to the simulated hydrogen burn environment was completed.

Prior to testing, the transmitter was pressurized at several differential pressures from 0 to 48.3 kPa (0 to 7 psi) and a performance curve obtained (Figure 8-10). Because of high pressure in the gas bottle the regulator could not maintain steady differential pressures below 20.7 kPa (3 psi) for this calibration check. The reading at 0 kPa was obtained by closing off the regulator and opening the bleed valve. The line on Figure 8-10 has the equation

$$V = 1.52 + 1.08P \quad (8-1)$$

where V = Signal Voltage
 P = Differential Pressure in psi

This equation was obtained using the linear regression program from a TI58 calculator and considering only differential pressures greater than 20.7 kPa (3 psi). It was decided to consider only these points because of their excellent consistency (correlation coefficient of 0.998). Normal procedure with this transmitter would be to adjust the signal to 2 volts at 0 kPa and 10 volts at 49.6 kPa (7.2 psi). (These pressure limits correspond to the Foxboro defined span of 0 to 200 inches of H₂O.) However, since the transmitter was to be tested at 7 psi differential pressure, the signal would have been very close to the 10 volt limit of the data acquisition system. Thus any but the most minor upward drifts in the signal would have been undetectable due to saturation of the data acquisition electronics. For this reason the calibration was allowed to remain as originally measured. Since the objective of the transmitter tests was to determine whether changes in performance occur as a result of hydrogen burns rather than to test absolute performance, allowing the calibration to remain in this state did not adversely effect the results.

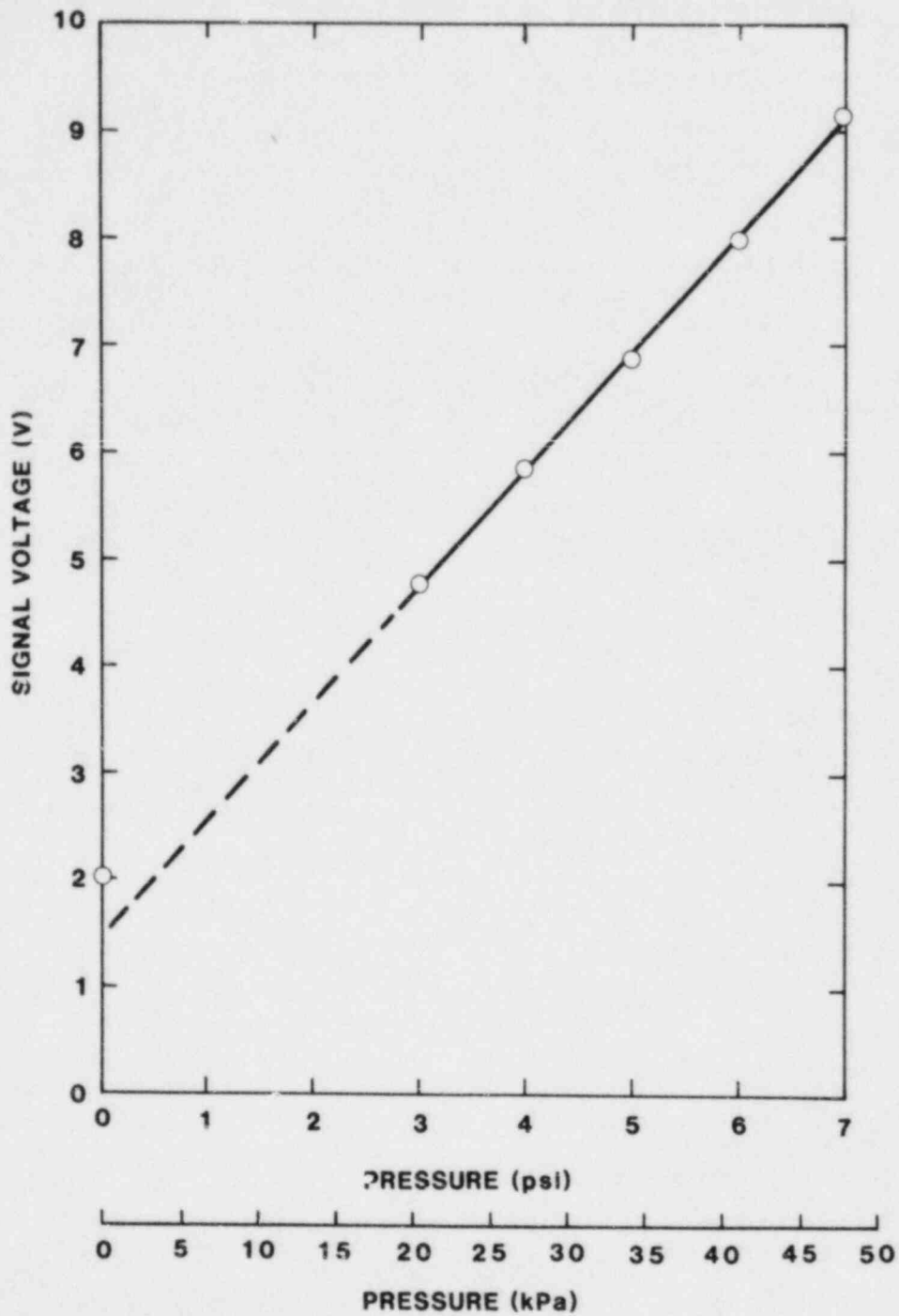


Figure 8-10 Foxboro Pretest Signal Output

Shortly after testing, a second calibration run was made. For this set of points the interior air temperature had dropped to 361 K (190°F). Results are shown in Figure 8-11. Lower bottle pressures allowed steady regulator operation down to 13.8 kPa (2 psi). Again, using the linear regression program the equation of the line was found to be

$$V = 0.40 + 1.23P \quad (8-2)$$

The correlation coefficient was again found to be 0.998. Comparison with the first curve (Figure 8-10) shows obvious changes in the calibration.

Several days later, after the instrument had had ample time to cool back to ambient conditions a third calibration run was made for comparison to the previous curves. Conditions for this run were the same as for the pretest calibration, interior air was at ambient temperature (293 K, 68°F). Results are shown in Figure 8-12. The equation for this line (disregarding the zero pressure point) is

$$V = 1.28 + 1.11P \quad (8-3)$$

and the correlation coefficient of the six data points considered was essentially 1 (i.e. greater than 0.9999). The three equations are summarized in Table 8-4 and all three graphs are compared in Figure 8-13.

Table 8-4

Foxboro Transmitter Calibration Equations

<u>Calibration Conditions</u>	<u>Equation</u>
Pretest, Ambient Temp	$V = 1.52 + 1.08P$
Posttest, 361 K/190°F	$V = 0.40 + 1.23P$
Posttest, Ambient	$V = 1.28 + 1.11P$

The indication here is that while cooling back to ambient conditions the instrument returned to a calibration closer to the pretest condition. A comparison of the instrument signal at 48.3 kPa (7 psi) for the three calibration runs and just prior to burn simulation (after preheating) is given in Table 8-5. From this comparison, it appears that the calibration change may have occurred during the preheat phase since the signal is lower from the outset of burn simulation.

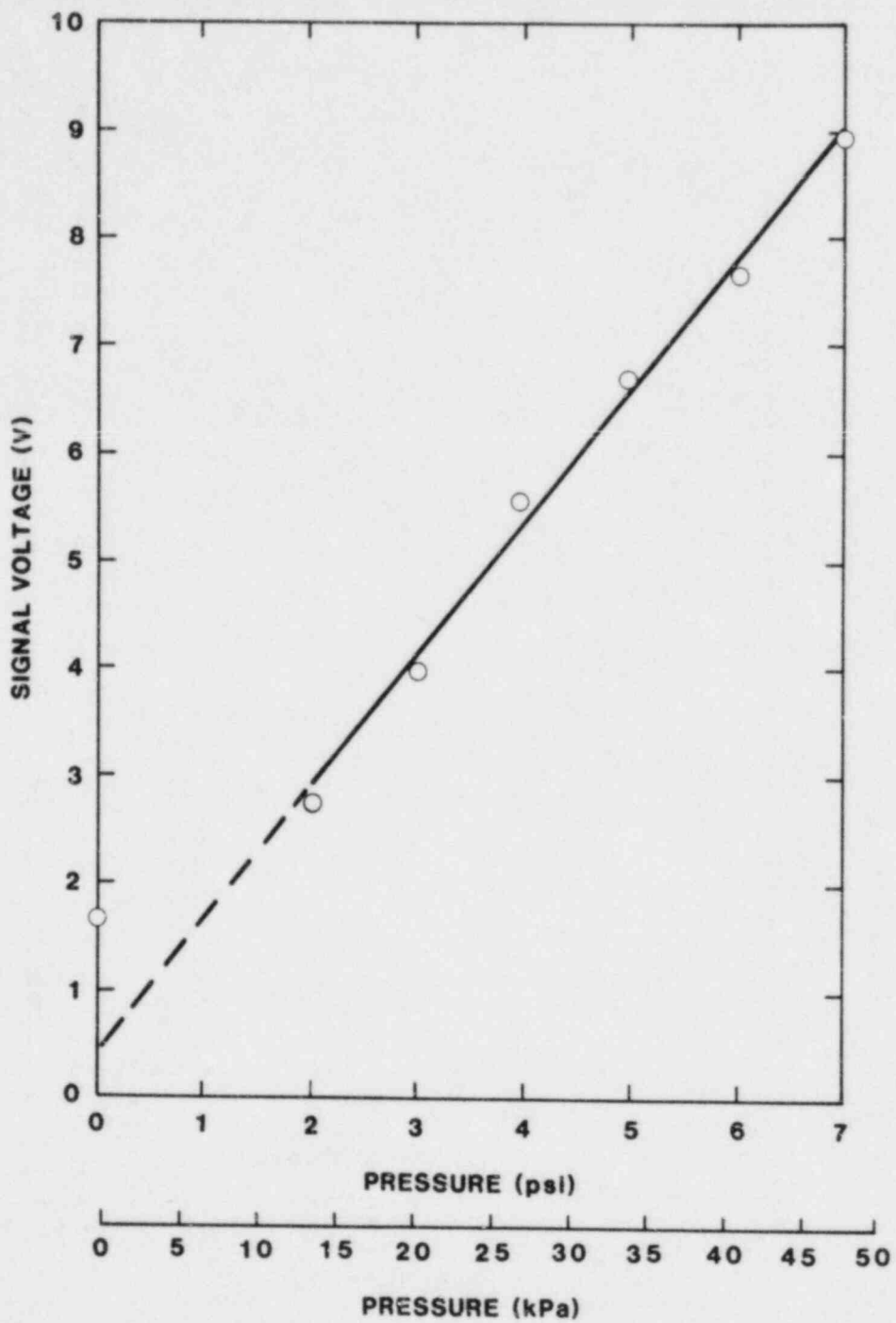


Figure 8-11 Foxboro Posttest Signal Output at Elevated Temperature

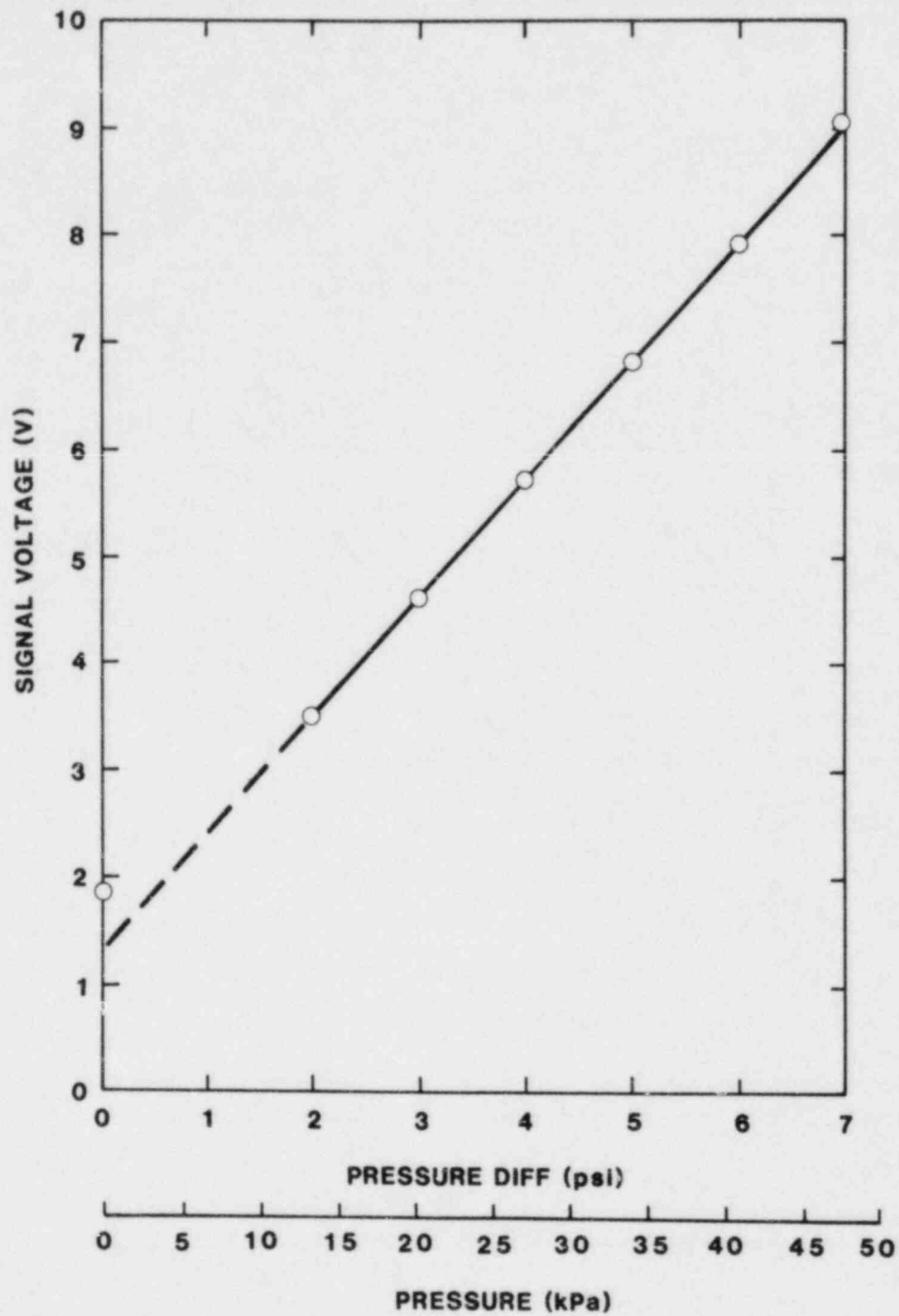


Figure 8-12 Foxboro Posttest Signal Output at Ambient Temperature

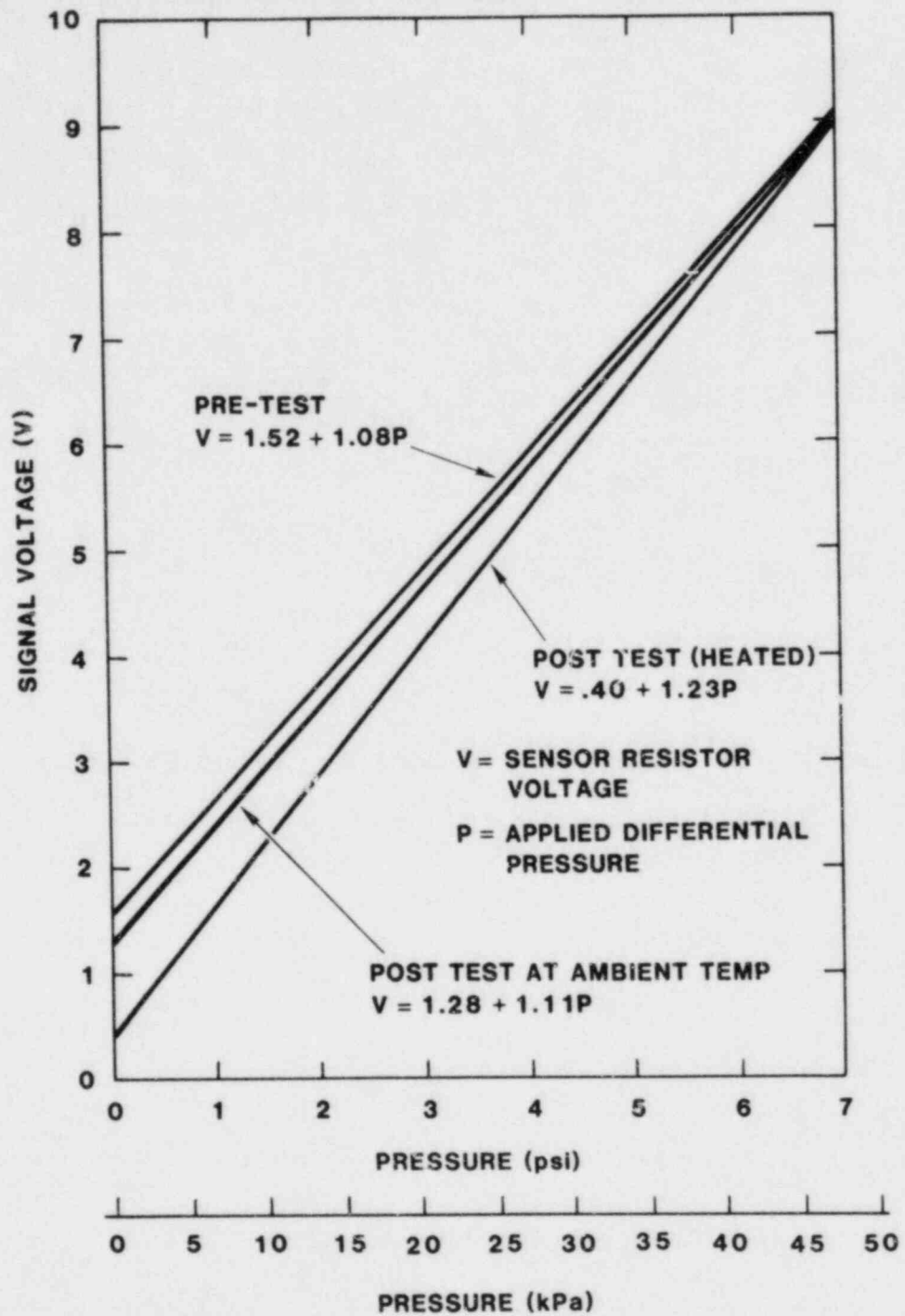


Figure 8-13 Foxboro Pre and Posttest Signal Comparison

Table 8-5

Foxboro Signal Comparison at
48.3 kPa (7 psi) Differential Pressure

Signal From	Interior Air Temperature (K/°F)	Signal	
		(V)	(mA)
Pretest	293/ 68	9.12	18.24
Burn Simulation Initiation	377/219	8.85	17.70
Posttest	361/190	8.91	17.82
Posttest	293/ 68	9.05	18.10

The first three entries of Table 8-5 are graphed in Figure 8-14. The equation of the line is

$$V = 10.05 - (3.177 \times 10^{-3})T \quad (8-4)$$

where V = signal voltage in volts

T = interior air temperature in K

While three data points are not very statistically significant, the correlation coefficient of -0.9995 indicates some trend in the calibration change may be present.

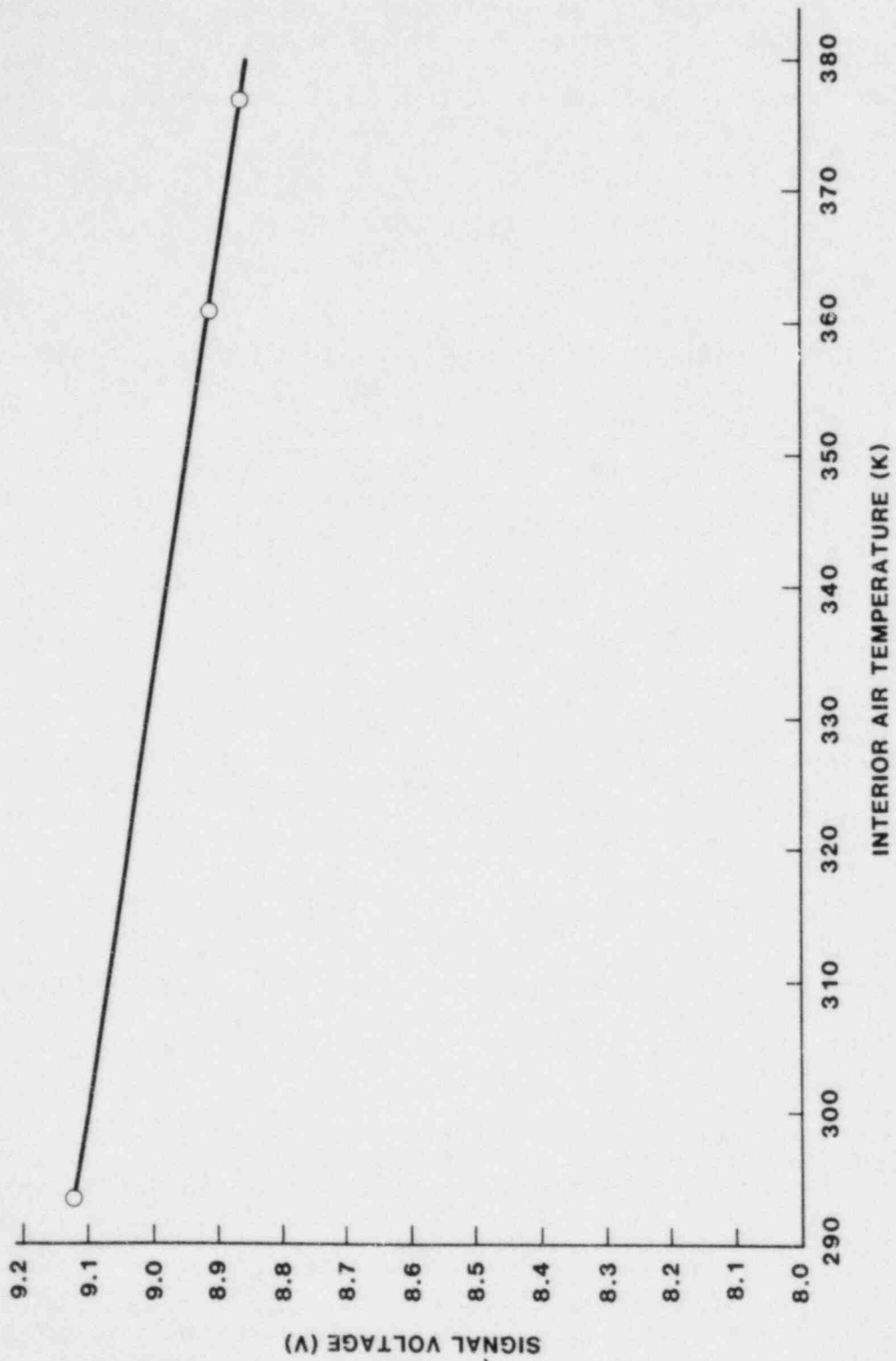


Figure 8-14 Effect of Temperature on Foxboro Signal Voltage
at Test Pressure (7psi)

8.6 Barton Pressure Transmitter

Prior to testing, two calibration curves were obtained for the Barton instrument. For the first, the interior air temperature was 291 K (64°F, ambient). The pressure range was from 0 to 20.7 MPa (0 to 3000 psi). The equation of the straight line for this calibration was

$$V = 1.81 + (2.61 \times 10^{-3})P \quad (8-5)$$

where V and P have the same definitions as for the Foxboro transmitter.

For the second pretest calibration the transmitter was heated slightly until the interior air temperature was 316 K (110°F). Using the same pressure range the equation of the calibration line was found to be

$$V = 1.85 + (2.59 \times 10^{-3})P \quad (8-6)$$

The two curves are virtually identical and are compared in Figure 8-15. The minor differences between the two curves can be attributed to slight differences in the regulator settings between the two calibration runs.

The zero reading for this instrument would normally be adjusted to 2 volts across the 500 ohm (nominal) resistor used for these tests. However, in order to allow for possible testing at pressures approaching the top of the transmitter range without threatening saturation of the data acquisition electronics it was decided to retain the slight offset for testing.

During testing the transmitter operated as designed. At a constant pressure of 15.5 MPa (2250 psi) the signal voltage was 7.68 v which is the same value obtained in the pretest calibrations. As shown in Figure 8-16 there is a slight fluctuation of 0.02 volts in the signal voltage which follows a fluctuation of 0.08 volts (from 1.58 to 1.66 volts) in the current amplifier output. Such a fluctuation in the signal corresponds to a change in pressure of 53 kPa (7.7 psi) or 0.3 percent of the applied pressure, an insignificant amount. Throughout the test the voltage reference power supply output remained steady at 6.5 volts.

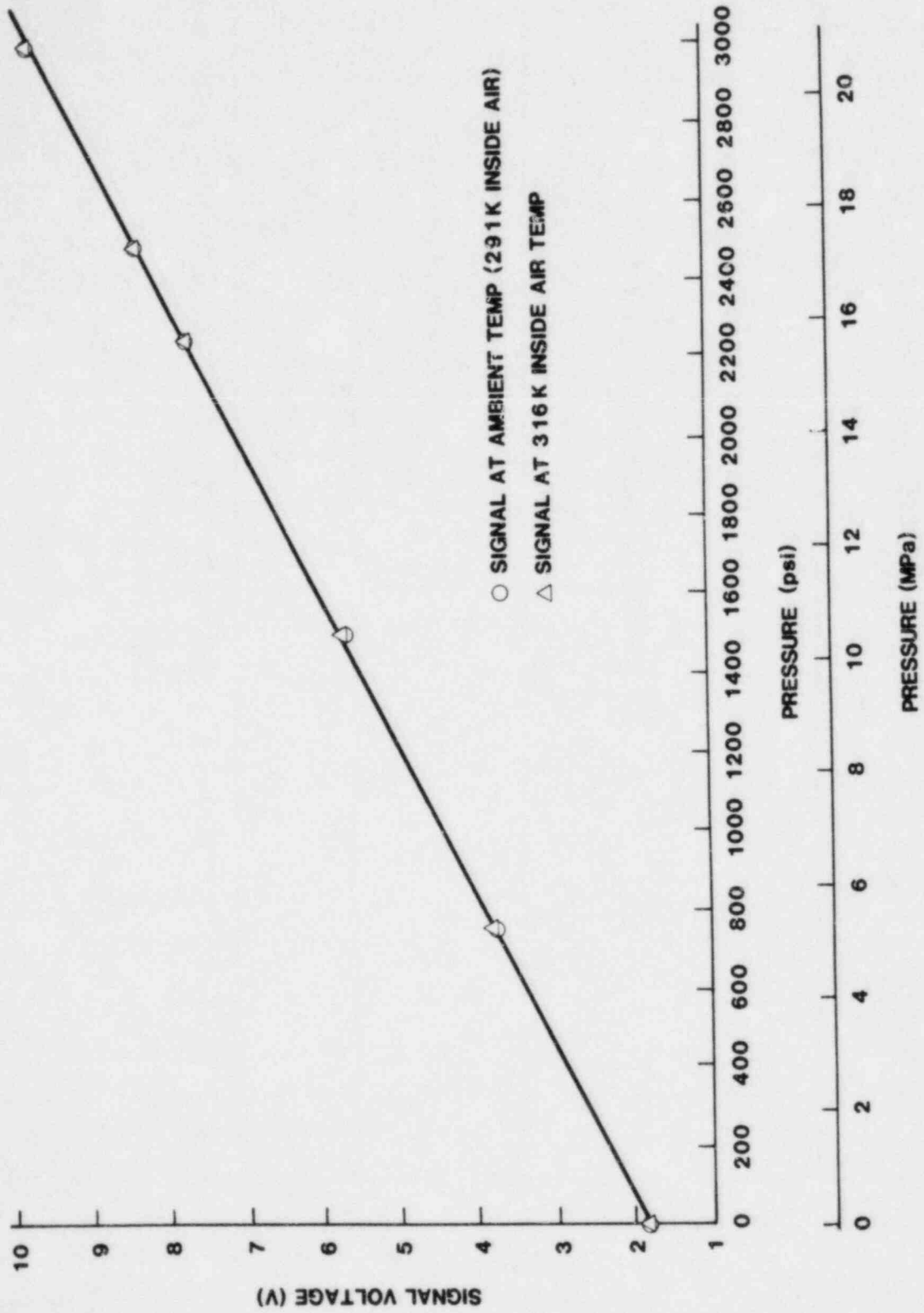


Figure 8-15 Pretest Barton Transmitter Calibrations

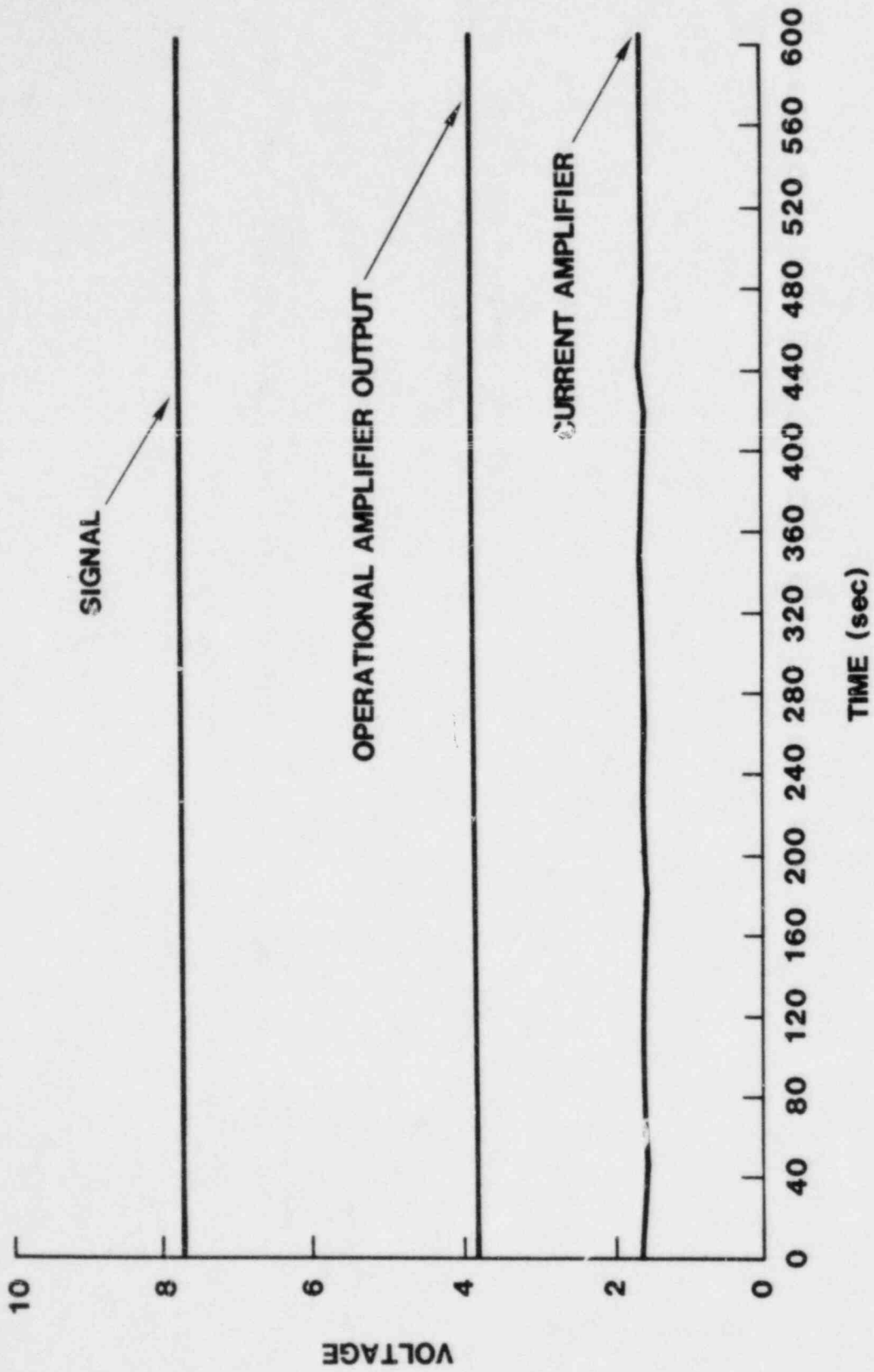


Figure 8-16 Barton Transmitter Voltages

Temperature responses of the casing and interior air are shown in Figure 8-17 and electronic component temperatures are shown in Figure 8-18. These temperature rises are summarized in Table 8-6.

Table 8-6

Barton Transmitter Temperature Rises

<u>Component</u>	<u>T_i</u> (K/°F)	<u>T_f</u> (K/°F)	<u>ΔT</u> (K/°F)
Casing Cover Plate (Face)	389/241	428/311	39/70
Casing Back	356/181	374/213	18/32
Interior Air	370/206	390/243	20/37
Noise Suppression Capacitor	367/201	381/227	14/26
Voltage Reg Pass Trans.	368/203	383/230	15/27
Current Amp Output Trans.	376/218	389/241	13/23

Immediately after testing, another series of calibration readings was taken. At the start of the readings the interior air temperature was 374 K (214°F). Over the time during which the readings were taken (approximately 10 minutes) this dropped to 360 K (188°F). The resulting calibration curve, shown in Figure 8-19, had an equation of

$$V = 1.89 + (2.55 \times 10^{-3})P \quad . \quad (8-7)$$

This equation compares well with the two pretest calibrations.

Several days later, after the instrument had cooled to ambient conditions, 293 K (68°F), still another calibration run was made. The curve, shown in Figure 8-20, had an equation of

$$V = 1.87 + (2.58 \times 10^{-3})P \quad . \quad (8-8)$$

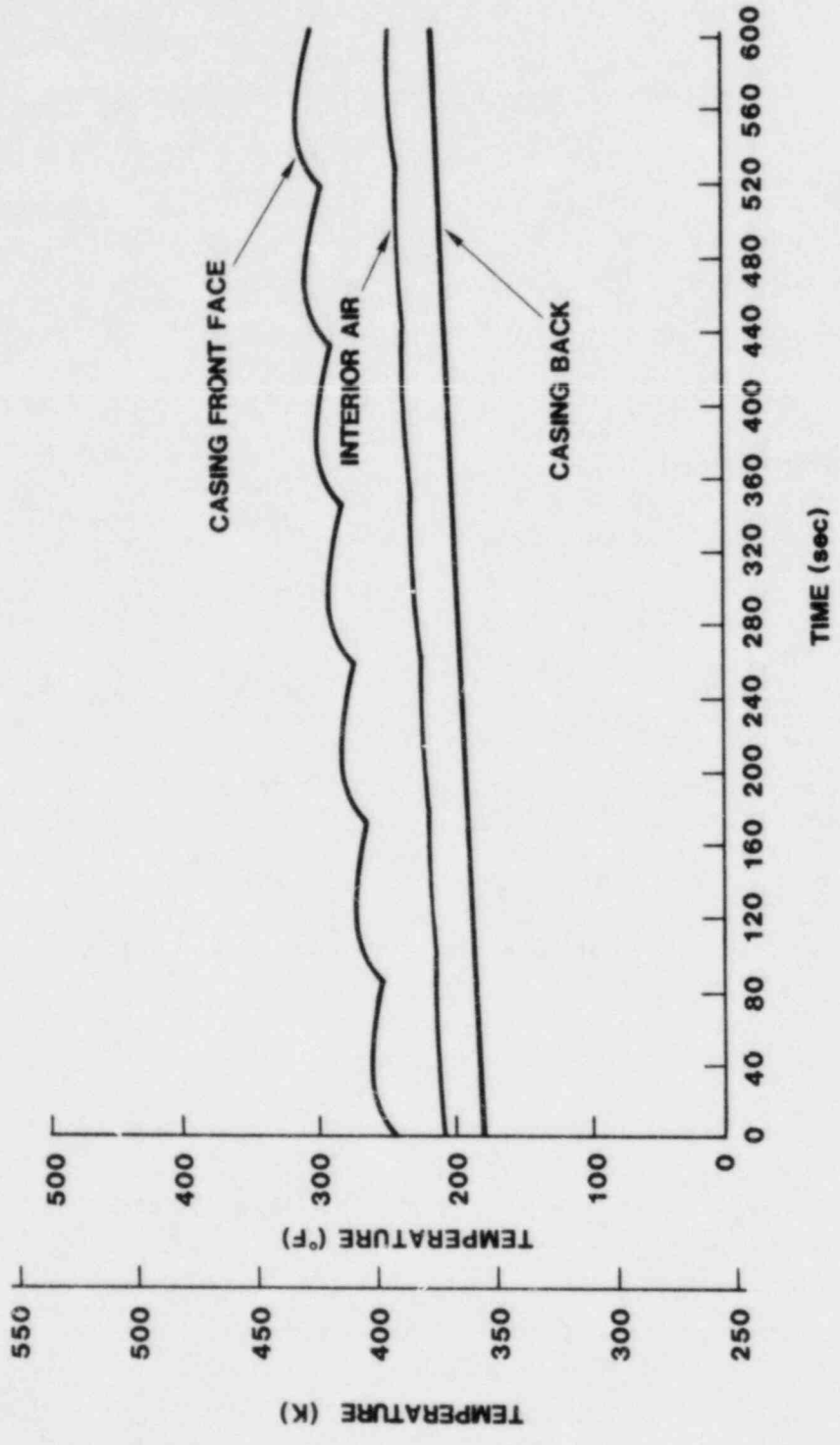


Figure 8-17 Barton Transmitter Casing Temperatures

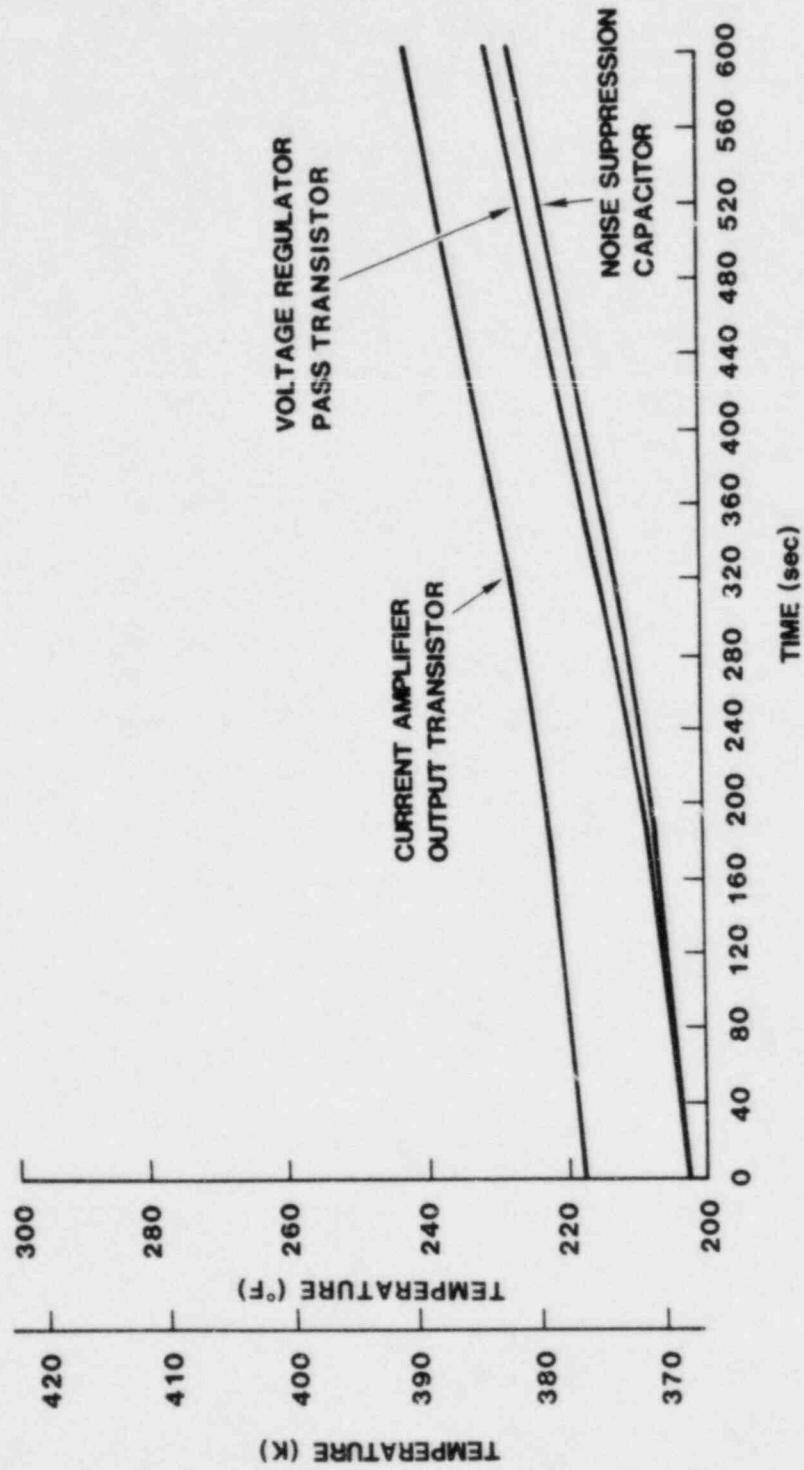


Figure 8-18 Barton Electronic Component Temperatures

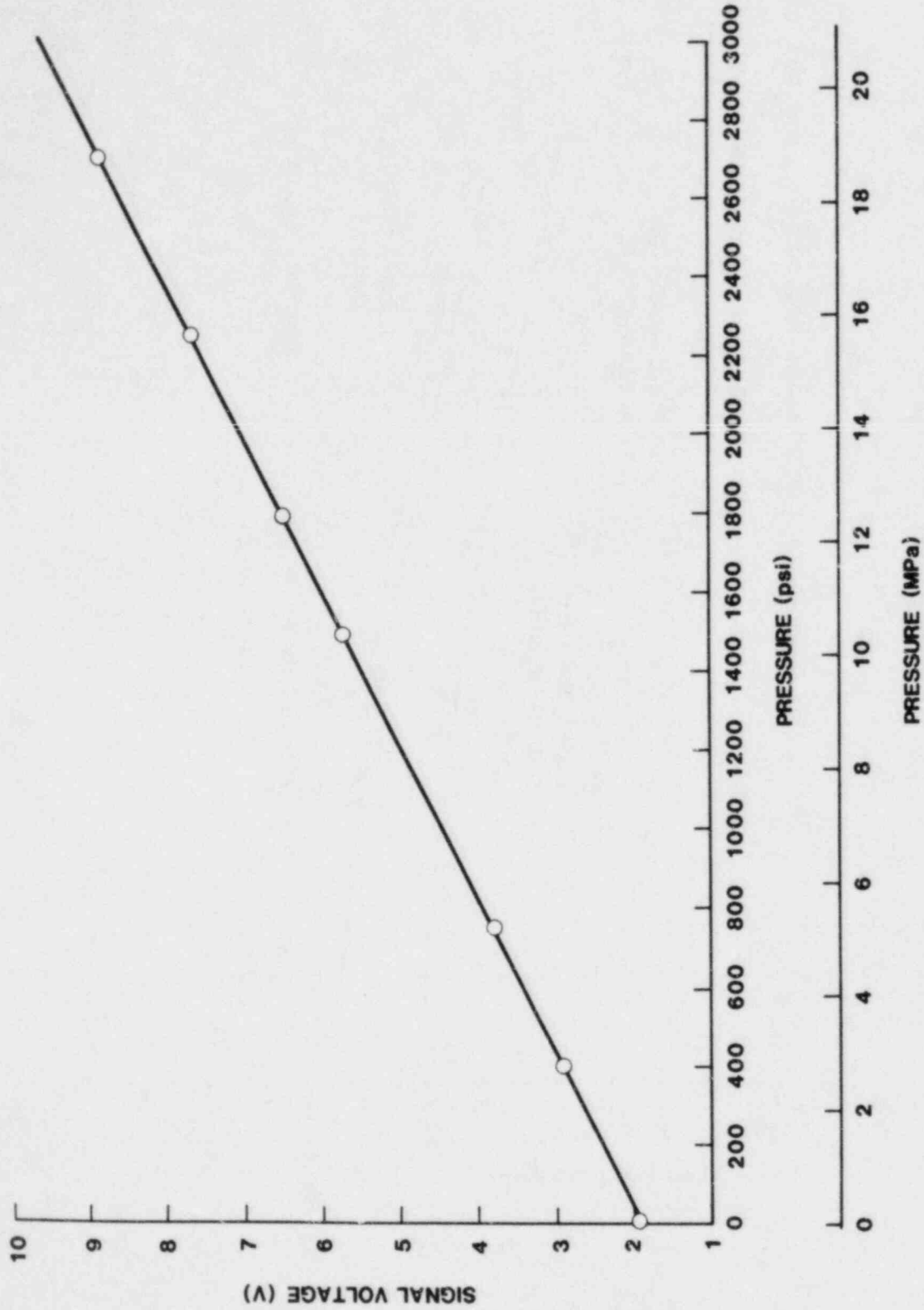


Figure 8-19 Posttest Barton Calibration at Elevated Temperature

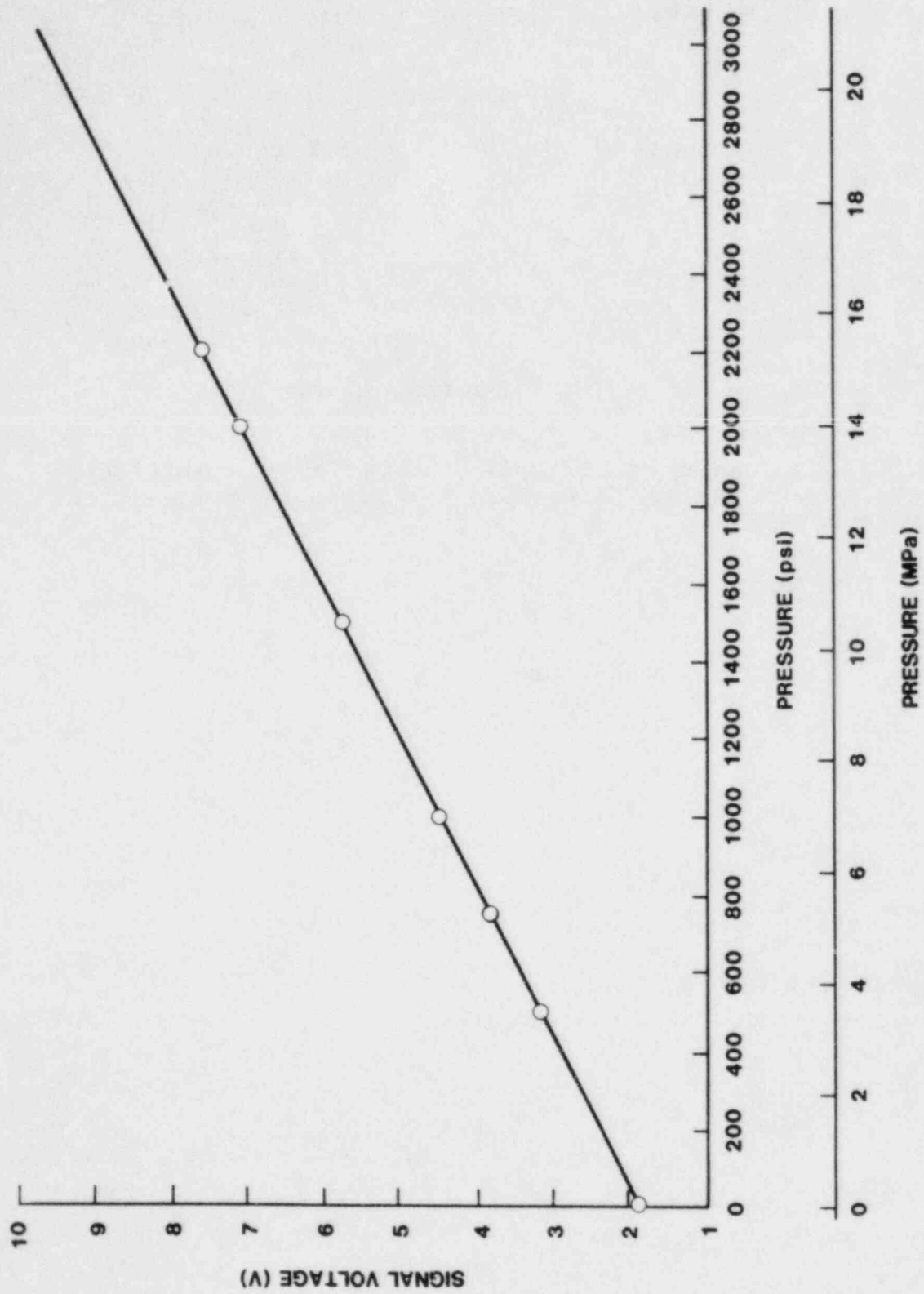


Figure 8-20 Posttest Barton Calibration at Ambient Temperature

Again, this agrees well with all previous calibrations. The equations of all four calibrations are summarized in Table 8-7 and the curves are compared in Figure 8-21.

Table 8-7

Barton Transmitter Calibration Equations

<u>Calibration Conditions</u>	<u>Equation *</u>
Pretest, Ambient Temp	$V = 1.81 + 0.00261P$
Pretest, 316 K/110°F	$V = 1.85 + 0.00259P$
Posttest, 374 K/214°F	$V = 1.89 + 0.00255P$
Posttest, Ambient Temp	$V = 1.87 + 0.00258P$

* V = signal voltage, P = pressure in psi

The slight differences in calibration can be attributed to slight uncertainties in reading the pressure gauge on the pressure regulator.

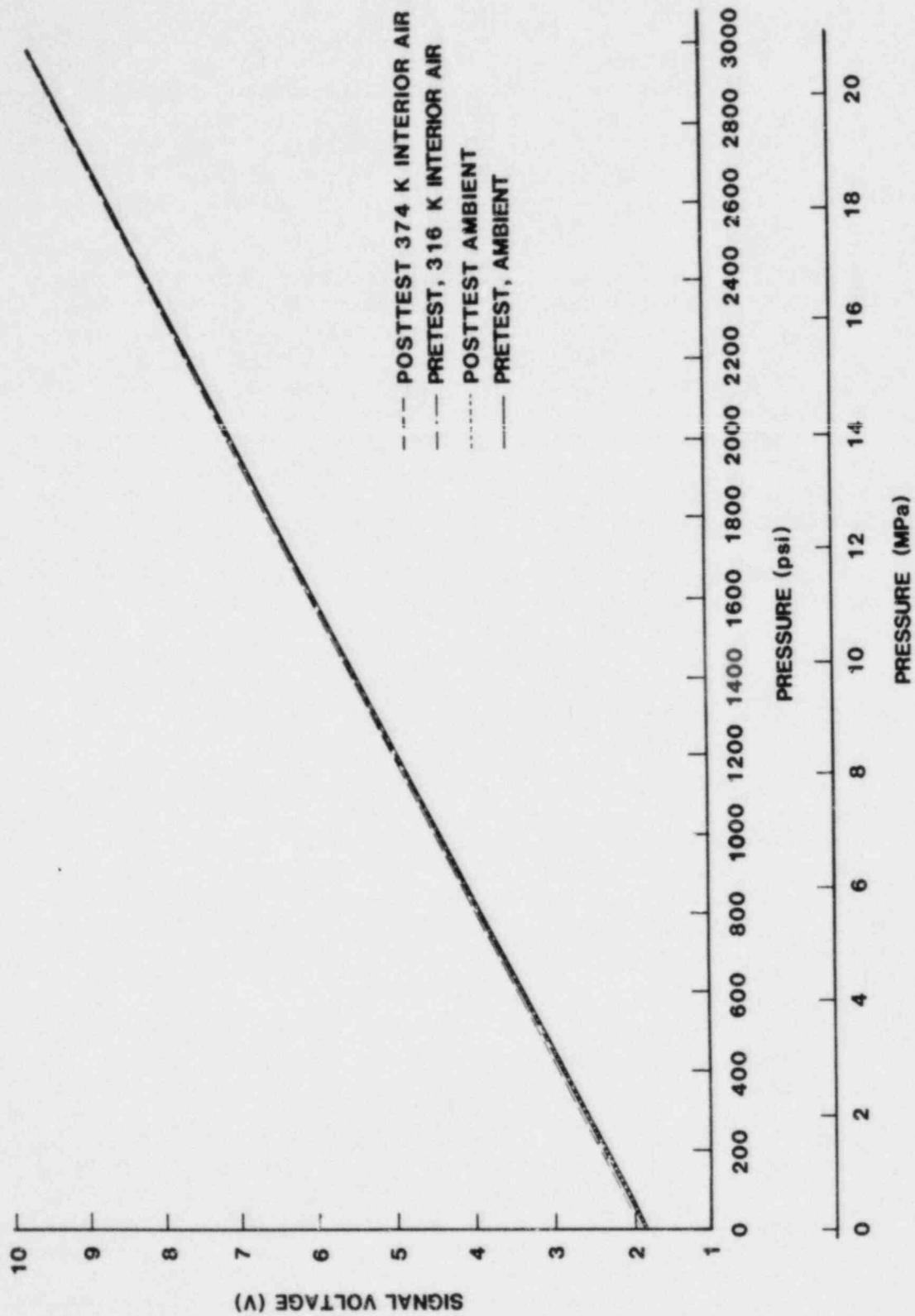


Figure 8-21 Barton Transmitter Calibration Comparison

9.0 Conclusions

The first objective of the CRTF tests was to develop the capability of the facility to simulate transient heat fluxes representative of hydrogen burns in full-scale containment volumes as defined by HECTR. For the first pulse of the string shown in Figure 4-1 the code predicted a temperature rise of 12.2 K for the cover plate of a Barton pressure transmitter. Several CRTF simulations of the same pulse resulted in an average temperature rise of 12.7 K in the same plate. This temperature rise takes place in a somewhat shorter time than predicted by HECTR because, though the heat input for the calculated and simulated pulses is the same, the CRTF pulse is shorter due to time and flux constraints dictated by the CRTF. This fact may partially account for the slightly higher temperature rise produced by the CRTF simulated pulse. This similarity in calculated and experimentally produced temperature rises for similar incident heat flux profiles indicates that the HECTR model of the cover plate can accurately predict the temperature response of that combination of geometry and material.

Multiple burns predicted by HECTR can be simulated by the repetition of a single pulse. The present series of tests used the pulse having the highest peak heat flux and longest duration. Testing with this pulse yields mildly conservative results for most specimens. Thus, in terms of heat flux and temperature response, the CRTF has been shown to represent the desired thermal environment.

It is again stressed that these experiments cannot be regarded as qualification tests. The CRTF does not have the capability of simulating the radioactive and moisture components of the severe accident environment. (These capabilities are, however, available at Sandia's Gamma Irradiation Facility¹⁰ and can be applied before or after a CRTF test as a given accident scenario dictates.) Nor does the facility reproduce the pressure pulses and shock waves associated with hydrogen combustion in closed volumes. The lack of pressure pulses is a minor point for the scenario considered since the maximum pressure calculated by HECTR was only 184.3 kPa (1.8 atm). The absence of shock waves has no bearing on the tests since they are associated with detonations rather than the deflagrations with which the HBS program is currently concerned. The slow heating of the equipment, due to environmental conditions prior to the hydrogen burn, was accomplished in a relatively rapid manner using a single heliostat. However, test specimens can be gradually heated to appropriate preburn temperatures, with minimal temperature gradients, using this method. Similarly, the air surrounding the test specimens is cooler than the containment atmosphere would be after a series of hydrogen burns. This condition causes outer surfaces of the test

specimens to cool more quickly than if they were in an actual containment. However, the temperature lag between component internals and the casing exterior is such that the difference in postburn and postsimulation atmospheric temperatures is not significant. In any case, these time-at-temperature factors are of concern only if the immediate preburn temperature or peak temperature (reached as a result of the hydrogen combustion) is significantly greater than the temperature to which the specimen has previously been qualified. At the present time the CRTF does not have the capability to irradiate samples from all sides simultaneously. However, equipment is often mounted on containment walls in much the same manner as the test specimens are mounted in the CRTF. Additionally, the scenario considered, while involving a severe thermal environment, has not yet been determined to be the bounding case for equipment survival in hydrogen burns. Also, the attachment of required test instrumentation in some cases necessitated partial disassembly of some test specimens. This might be interpreted as having compromised the qualified status of those test specimens.

Though these limitations must be recognized, several useful conclusions pertaining to equipment performance can be drawn from the present test series. General results for all test specimens are summarized in Table 9-1.

LOCA qualification temperatures are normally in the vicinity of 440 K (332°F). The only components to exceed this temperature were the front doors of the large NEMA box and the similar but smaller NEMA enclosure of the hydrogen ignitor assembly. This is not unexpected considering the sheet metal construction of the boxes and their consequent small thermal masses. However, interior environments of the enclosures are such that components housed in them would not reach the LOCA temperature. This is borne out by the maximum temperatures of the air in the large box and the core of the hydrogen ignitor transformer.

Other more massive test specimens did not exceed the 440 K level. Even with the added component of electrical heating, transistors in the pressure transmitters did not approach the temperature at which aberrations in performance might be expected to occur (approximately 450 K or 350°F).

Both solenoid valves performed well with no valve sticking or electrical failure. This is particularly significant in the case of the FITS valve which had been subjected to severe environments in a previous test series which involved not only hydrogen combustion but also large amounts of moisture in the form of steam and condensate.

Table 9-1

Generalized Results of CRTF Hydrogen Burn Simulation

<u>Specimen</u>	<u>T_{max} (K)</u>	<u>Results</u>
<u>NEMA BOX</u>	475	No apparent damage
<u>Cables</u>		
Qualified 1		Slight discoloration on jacket of Qualified 1; all 4 samples maintained continuity; no current leakage; small bubble formed in jacket of unqualified sample.
Qualified 2		
Qualified 3		
Unqualified		
<u>Terminal Blocks</u>		
No apparent physical damage or electrical degradation.		
<u>Hydrogen Igniter</u>		
Box	494	No apparent damage Constant voltage output
Transformer	400	
<u>ASCO Solenoid Valve</u>		
Solenoid Housing	422	Continued cycling with no interruption.
Valve Body	344	
<u>Barton Pressure Transmitter</u>		
Casing	428	Steady pressure signal No appreciable calibration change.
Transistor	389	
<u>Foxboro Pressure Transmitter</u>		
Casing	399	Steady pressure signal, change in calibration after testing.
Transistor	384	

Both transmitters performed well during testing at pressures set near the upper end of their respective operating ranges. The Barton Model 763 pressure transmitter remained in the same state of calibration throughout testing. The Foxboro N-E13DM instrument showed minimal change in operational characteristics when operated at 48.3 kPa (7 psi).

The calibration changes which occurred in the Foxboro instrument warrant further investigation if the differential pressure being monitored is near the lower end of the operating range and the transmitter is at elevated tempera-

tures. At the test pressure (7 psi) the signal differed from the pretest calibration by about 0.8 percent. At 20.7 kPa (3 psi) however, the difference is 22 percent. The high correlation coefficients of the readings imply that the instrument calibration is changing in some predictable manner. This is further evidenced by the trend in signal decline shown in Figure 8-14 which compares the measured signal to the interior air temperature at the applied test pressure. The principle of operation of the transmitter⁹ is such that thermal expansion in the levers and rods of the force motor might account for this. This possibility has not been investigated.

It is also evident from the Foxboro calibration curves (Figures 8-10 to 8-12) that the reading at zero pressure does not fall on the line that is so well defined by data by the data above 20.7 kPa (3 psi). The circuitry of the device is such that the output signal should be proportional to the applied differential pressure regardless of the calibration set points at the extremes of the operating range.¹¹ In a report on unrelated testing of Foxboro transmitters an anomaly was considered as having occurred when "with the application of a measured pressure or differential pressure, a proportional electrical signal is not produced."¹² Thus, in the CRTF tests, anomalous behavior did occur at zero applied differential pressure. The referenced report also indicates that calibration changes similar to those noted here occurred when specimens were subjected to environments which would produce much higher component temperatures than those encountered in these tests.

According to Reference 9, the upper operating limit of the instrument is reached when the topworks (cover) reaches a temperature of 394 K (250°F) and the peak LOCA transient limit is 436 K (325°F) for 10 minutes. The CRTF sample peak temperature reached 399 K (258°F), slightly above the operating limit but well below the transient limit and immediately after reaching its peak started to decline. There is also an indication that the change in calibration may have occurred prior to the burn simulation. Table 8-5 shows a signal of 8.85 volts (compared to the 9.12 volt pretest calibration value) at test pressure. This reading was taken just after preburn simulation heating was completed when the instrument air temperature was 377 K (219°F) and the casing temperature was 390 K (242°F), a temperature below the operating limit. The test pressure was 7 psi (differential), which is very near the top of the instrument's operating range. The 8.85 volt signal differs from the pretest calibration value of 9.12 volts by slightly less than 3 percent. The posttest calibration showed that this difference became increasingly larger at lower differential pressures. At 3 psi (differential) the difference was approximately 20 percent.

From these results it is concluded that the mechanisms causing calibration changes in the Foxboro N-E13DM differential pressure transmitter should be investigated. This is especially necessary if the instrument is being considered for applications at differential pressures at the low end of its operational span.

With the caveat that the Foxboro transmitter be operated at the upper end of its differential pressure range, it can generally be concluded that, in terms of equipment response, the thermal environment in the lower compartment of an ice condenser containment resulting from a hydrogen burn sequence precipitated by an S₂D accident does not, by itself, appear to threaten safety-related equipment having thermal characteristics similar to the specimens considered in this series of tests.

References

1. H. Alvares, D. Bearson, and G. Eidem, Investigation of Hydrogen Burn Damage in the Three Mile Island Unit 2 Reactor Building, GEND-INF-023, Vol 1, U.S. Department of Energy, June 1982.
2. W. H. McCulloch, et al., Hydrogen Burn Survival: Preliminary Thermal Model and Test Results, SAND82-1150; NUREG/CR-2730, August 1982.
3. J. T. Holmes, et al., Central Receiver Test Facility (CRTF) Experiment Manual, SAND77-1173-revised, October 1979.
4. A. L. Camp, et al., MARCH-HECTR Analysis of an Ice Condenser Containment, SAND83-0501C, Proceedings of the International Meeting on LWR Severe Accident Evaluation (August 28 - September 1 1983)
5. Memo: A. M. Kolaczowski (SNLA, 9412) to W. H. McCulloch, (SNLA 9445) dated 2-9-83, subject: Request on Accident Sequence Probabilities for H₂ Study.
6. Memo: A. R. Mahoney and R. B. Pettit (SNLA, 1824) to V. J. Dandini (SNLA, 9445), dtd 12-6-82, subject: Optical Properties Measurements of Valve Assembly and Various Gray Parts.
7. F. Biggs and C. N. Vittitoe, The HELIOS Model for the Optical Behavior of Reflecting Solar Concentrators, (SAND76-0347), Sandia National Laboratories, March 1979.
8. E. H. Richards and J. J. Aragon, Hydrogen Burn Survival Experiments at FITS, SAND83-1715, in preparation.
9. The Foxboro Company, Instruction Book for N-E11 and N-E13 Electronic Transmitters, 1982.
10. Letter: L. L. Bonzor (SNLA, 9446) to W. S. Farmer (USNRC), dated 5-26-83, subject: Elastomer-Covered Flexible Metal Hose Test Experiences.
11. Private conversation with David T. Furgal (SNLA, 6445) 9-23-83.
12. Wyle Laboratories, Nuclear Environmental Qualification Test Program on Foxboro N-E10 Series Pressure Transmitters, Vol I, May 1983.

Distribution

U.S. Nuclear Regulatory Commission
Distribution Contractor (CDSI)
15700 Crabbs Branch Way
Rockville, MD 20850
100 copies for AN Distribution Code

U.S. Nuclear Regulatory Commission
Office of Nuclear Regulatory Research
Division of Engineering Technology
Washington, DC 20555
Attn: William Farmer (5)

U.S. Nuclear Regulatory Commission
Office of Nuclear Regulatory Research
Division of Accident Evaluation
Washington, DC 20555
Attn: J. T. Larkins

U.S. Nuclear Regulatory Commission
Office of Nuclear Reactor Regulation
Division of Engineering
Washington, DC 20555
Attn: K. I. Parczewski

F. Gregory Hudson
Duke Power Company
Design Engineering Dept.
P.O. Box 33189
Charlotte, NC 28242

Claire Meser
Energy Incorporated
1 Energy Drive
Box 736
Idaho Falls, ID 83402

Dr. S. F. Hall
Safety and Reliability Directorate
United Kingdom Atomic Energy Authority
Wigshaw Lane
Culcheth
Warrington WA34NE, Cheshire
Great Britain

Engineering Planning and Management
298 Boston Post Road
Wayland, MA 01778
Attn: Phil Holzman

Dr. Stanley Turner
Southern Science Applications
P.O. Box 10
Dunedin, FL 33528

Mr. Lasse Reiman
Department of Reactor Safety
Institute of Radiation Protection
P.O. Box 268
00101 Helsinki 10
Finland

Dr. M. McIntyre
Technical Department
Rolls-Royce & Associates Ltd.
P.O. Box 31
Derby, DE2 8BJ
Great Britain

Dr. Werner Baukal
Battelle-Institut e.V.
Am Röwershof 35
D-6000 Frankfurt am Main 90
Federal Republic of Germany

1512 J. C. Cummings
1513 S. N. Kempka
1513 A. C. Ratzel
2513 S. F. Roller
2513 J. E. Shepherd
3141 C. M. Ostrander (5)
3151 W. L. Garner
6400 A. W. Snyder
6425 W. Frid
6427 M. Berman
6427 B. Marshall
6427 S. E. Dingman
6440 D. A. Dahlgren
6442 W. A. von Rieseemann
6444 S. L. Thompson
6445 J. J. Aragon (6)
6445 V. J. Dandini (12)
6445 D. T. Furgal
6445 D. B. King
6445 W. H. McCulloch (6)
6445 E. H. Richards
6446 L. L. Bonzon
6447 D. L. Berry
6449 K. D. Bergeron
8424 M. A. Pound

NRC FORM 336 (2-84) NRCM 1102 3201, 3202		U.S. NUCLEAR REGULATORY COMMISSION		REPORT NUMBER (Assigned by T/DC and Vol. No. if any) NUREG/CR-3776 SAND83-1960	
SEE INSTRUCTIONS ON THE REVERSE					
2 TITLE AND SUBTITLE Testing of Safety-Related Nuclear Power Plant Equipment at the Central Receiver Test Facility			3 LEAVE BLANK		
5 AUTHOR(S) Vincent J. Dandini John J. Aragon			4 DATE REPORT COMPLETED MONTH: July YEAR: 1984		6 DATE REPORT ISSUED MONTH: July YEAR: 1984
7 PERFORMING ORGANIZATION NAME AND MAILING ADDRESS (Include Zip Code) Safety Systems Assessment Division (6445) Sandia National Laboratories P.O. Box 5800 Albuquerque, NM 87185			8 PROJECT TASK WORK UNIT NUMBER N/A		
10 SPONSORING ORGANIZATION NAME AND MAILING ADDRESS (Include Zip Code) Division of Accident Evaluation, Office of Nuclear Regulatory Research and Division of Engineering, Office of Nuclear Reactor Regulation, U.S. Nuclear Regulatory Commission Washington, DC 20555			9 FIN OR GRANT NUMBER Fin No. A-1270 Fin No. A-1306		11a TYPE OF REPORT Final, Technical
12 SUPPLEMENTARY NOTES					
13 ABSTRACT (200 words or less) <p>The use of a solar energy facility for simulating the thermal environment (heat flux) produced as a result of hydrogen burns in a full-scale reactor containment building is described. Using a heat flux profile developed from calculations performed by the HECTR computer code, the Central Receiver Test Facility simulated the multiple burn thermal environment which HECTR predicted would result from the deliberate ignition of hydrogen generated by an S₂D accident. Functioning specimens of reactor monitoring and safety system equipment were exposed to this environment. Results of the equipment performance and temperature response are presented.</p>					
14 DOCUMENT ANALYSIS - KEYWORDS DESCRIPTORS Reactor Instrumentation, Reactor Accidents, Reactor Protection Systems				15 AVAILABILITY STATEMENT Unlimited	
16 IDENTIFIERS/OPEN ENDED TERMS Hydrogen Burr, Equipment Survivability, Pressure Transmitters, Solenoid Valves				16 SECURITY CLASSIFICATION (This page) Unclassified (This report) Unclassified	
				17 NUMBER OF PAGES	
				18 PRICE	

